DISSERTATIONES CHIMICAE UNIVERSITATIS TARTUENSIS

96

DISSERTATIONES CHIMICAE UNIVERSITATIS TARTUENSIS
96

LIIS SIINOR

Adsorption kinetics of ions at Bi single crystal planes from aqueous electrolyte solutions and room- temperature ionic liquids

TARTU UNIVERSITY
PRESS

Institute of Chemistry, Faculty of Science and Technology, University of Tartu, Estonia

Dissertation is accepted for the commencement of the Degree of Doctor of Philosophy in Chemistry on June 21st, 2010 by the Council of Institute of Chemistry, University of Tartu.

Supervisors: Prof. Enn Lust, University of Tartu

Ph.D. Karmen Lust, University of Tartu

Opponents: Prof. Renat Nazmutdinov,
Kazan State University, Kazan, Tatarstan, Russia.

Prof. Andres Öpik,
Tallinn University of Technology, Estonia

Commencement: August, 24th, 2010, Ravila 14A (Chemicum), room 1021, 12.00

Euroopa Liit
Euroopa Sotsiaalfond

Eesti tuleviku heaks

ISSN 1406–0299
ISBN 978–9949–19–416–2 (trükis)
ISBN 978–9949–19–417–9 (PDF)

Tartu Ülikooli Kirjastus
www.tyk.ee
Tellimus nr. 387

to my dearest ones

CONTENTS

1. LIST OF ORIGINAL PUBLICATIONS 8
   Author´s contribution: 8
2. ABBREVIATIONS AND SYMBOLS 9
3. INTRODUCTION 11
4. LITERATURE OVERVIEW 12
   4.1 Adsorption kinetics of ions on single crystal electrodes 12
   4.2 Ionic liquids 13
      4.2.1 Physical properties of ionic liquids [35–36] 13
      4.2.2 Ionic liquids in electrochemistry 14
   4.3 Electrochemical impedance spectroscopy 15
   4.4 Cyclic voltammetry 17
5. EXPERIMENTAL 19
   5.1 Measurements in aqueous solutions 19
   5.2 Measurements in ionic liquids 19
6. RESULTS AND DISCUSSION 20
   6.1 Adsorption of iodide ions at Bi(111) and Bi(001) single crystal electrodes 20
      6.1.1 Analysis of impedance data 23
   6.2 Properties of electrical double layer at Bi(111) | ionic liquid interface 27
      6.2.1 Simulation of impedance data 31
   6.3 Comparison of limiting stages of adsorption and some characteristic parameters of ionic liquids and aqueous solutions of KI at Bi(111) and Bi(001) 33
      6.3.1 Analysis of limiting stages of adsorption 33
      6.3.2 Similarity and analysis of Nyquist plots 34
7. SUMMARY 36
8. REFERENCES 37
9. SUMMARY IN ESTONIAN 40
10. ACKNOWLEDGEMENTS 41
11. PUBLICATIONS 43

1. LIST OF ORIGINAL PUBLICATIONS

I. **L. Siinor**, K. Lust and E. Lust, Impedance study of adsorption of iodide ions at Bi(001) electrode from the aqueous solutions with constant ionic strength, Journal of Electroanalytical Chemistry, Volume 601, Issues 1–2, 15 March 2007, Pages 39–46.

II. **L. Siinor**, V. Ivaništšev, K. Lust, E. Lust, Impedance study of adsorption of iodide ions at Cd(0001) and Bi(111) electrode from various solutions with constant ionic strength, Journal of Solid State Electrochemistry, Volume 14, Number 4, April, 2010, Pages 555–563.

III. **L. Siinor**, K. Lust, and E. Lust, Electrical Double Layer Structure at Bi(111)|1-ethyl-3-methyl-imidazolium Tetrafluoroborate Interface, ECS Transactions, Volume 16 , Issue 49, October 2008, Pages 559–567.

IV. **L. Siinor**, K. Lust, E. Lust, Electrical Double Layer Capacitance at Bi(111)|1-Ethyl-3-methylimidazolium Tetrafluoroborate Interface as a Function of the Electrode Potential, Journal of Electrochemical Society, Volume 157, Issue 7, 25 May 2010, Pages F83–F87.

V. **L. Siinor**, K. Lust, E. Lust, Influence of anion composition and size on the double layer capacitance for Bi(111) | room temperature ionic liquid interface, Electrochemistry Communications, Article in Press.

Author's contribution:

Paper I: Performed all electrochemical measurements, modeling of data and interpretation of results.
Paper II: Performed all electrochemical measurements at Bi(111) electrode, modeling of data and interpretation of results.
Paper III: Performed all electrochemical measurements, modeling of data and interpretation of results.
Paper IV: Performed all electrochemical measurements, modeling of data and interpretation of results.
Paper V: Performed all electrochemical measurements, modeling of data and interpretation of results.

2. ABBREVIATIONS AND SYMBOLS

A	CPE coefficient
A	area of the electrode
ac	alternating current
AFM	atomic force microscopy
c	analyte concentration
C_0	thermodynamic low-frequency capacitance
C_{ad}	adsorption capacitance
C_{dl}	"true" high-frequency differential double layer capacitance
c_{KI}	concentration of KI
CPE	constant phase element
C_{s}	differential capacitance
CV	cyclic voltammetry
D	diffusion coefficient
E	electrode potential
EC	equivalent circuit
edl	electrical double layer
EDLC	electrochemical double layer capacitor
EIS	electrochemical impedance spectroscopy
$\mathrm{EMImBF_4}$	1-ethyl-3-methylimidazolium tetrafluoroborate
EMImFAP	1-ethyl-3-methylimidazolium tris(pentafluoroethyl)trifluorophosphate
EMImTCB	1-ethyl-3-methylimidazolium tetracyanoborate
E_{min}	potential of minimum in C, E- curves
f	ac frequency
FMG	Frumkin-Melik-Gaikazyan model
j	imaginary unit, $\mathrm{j} = \sqrt{-1}$
IL	ionic liquid
i_{p}	peak current
ISE	ion selective electrode
j	current density
n	number of moles
q	electrode charge density
R_{ad}	adsorption (or partial charge transfer) resistance
R_{D}	diffusion-like process resistance
R_{el}	high-frequency series resistance
R_{p}	parallel resistance
RTIL	room temperature ionic liquid
SCE	saturated calomel electrode
STM	scanning tunneling microscopy
Z	complex impedance
Z'	real part of the impedance
Z''	imaginary part of the impedance

Z_w	Warburg-like diffusion impedance
$Z_{\mathrm{W(oc)}}$	open circuit finite length Warburg impedance
T	mass transfer frequency factor
v	potential scan rate
x	mole fraction of KI
χ^2	chi-square function
μ	chemical potential
Γ	Gibbs adsorption
α	CPE fractional exponent
σ_ad	Warburg constant
τ_D	diffusion relaxation time
τ_H	adsorption relaxation time
(hkl)	the notation of the Bi crystallographic plane (index)
$\|Z\|$	impedance modulus
δ	phase angle
Δ^2	weighted sum of squares
ΔE	potential region of ideal polarizability

3. INTRODUCTION

Adsorption of various ions and molecules has been elaborately studied by several groups of electrochemists. Adsorption processes effect crucially characteristics of heterogeneous electrochemical processes such as anodic dissolution, electrochemical corrosion, electrodeposition, electrosynthesis and electroanalysis of ions and molecules and also processes in electric double layer capacitors and fuel cells. Nature of surface active substances as well as ingredients of solutions and crystallographic structure of electrode surface affect significantly the adsorption process in electrical double layer. Therefore the adsorption kinetics and thermodynamics of inorganic and organic ions, neutral molecules on metal electrodes (poly- and mono crystalline), as well as at the porous carbon electrodes from aqueous and nonaqueous solutions have been studied.

The reason of specific adsorption of anions is the strong interaction between partly desolvated anion and surface atoms of metal. At certain positive surface polarization it leads to the formation of covalent bond between anion and metal surface, which is the slow process and limiting stage is the charge transfer or adsorption step.

Formation of the compact adsorption layer of aromatic heterocyclic polyfunctional compounds with specifically adsorbed cations can be used as an effective corrosion inhibitor. The process of electrosynthesis is strongly affected by the composition of surface inactive electrolyte selected as well as by presence of cations and anions that adsorb specifically.

To date, most electrochemical reactions have been carried out in the electrolytes of molecular solvents. Recently, however, a new class of electrolytes has emerged – ionic liquids. These electrolytes are fluid at room temperature, and consist mainly of ionic species. They have many fascinating properties which make them of fundamental interest to all chemists, since both the thermodynamics and kinetics of reactions carried out in ionic liquids are different to those in conventional electrolytes of molecular solvents. As they are made up of at least two components which can be varied (the anion and cation), these electrolytes can be designed with a particular end use in mind, or to possess a particular set of properties. The use of non-aqueous electrolytes and room temperature ionic liquids in electrochemical double layer capacitors (EDLC) was initiated by the wider region of ideal polarizability of nanoporous carbon | electrolyte interface in comparison with the traditional aqueous electrolyte solutions.

The main aim of this work was to establish the limiting stages for the adsorption process and to calculate the kinetic parameters describing iodide ions adsorption at Bi(111) and Bi(001) electrodes from aqueous binary electrolyte solutions as well as to analyze the electrical double layer structure at Bi(111) | ionic liquid interface.

4. LITERATURE OVERVIEW

4.1 Adsorption kinetics of ions on single crystal electrodes

Adsorption of the halide ions from aqueous and non-aqueous electrolyte solutions on single crystal plane electrodes of various metals has been investigated by several electrochemists for a long time [1–21]. However, there are only few works devoted to the adsorption kinetics of the halide and other anions on various single crystal plane electrodes – Au(*hkl*), Ag(*hkl*), Pt(*hkl*), Rh(111) – from aqueous electrolyte solutions and on Bi(*hkl*) from non-aqueous electrolyte solutions [1–6]. The adsorption of halide ions as well as other anions seems to be a rather complicated process [1–33] and the structure of the adsorption layer depends noticeably on the electrode potential, chemical composition and concentration of ions and on the nature of the metal as well as solvent studied [5,6]. At Au (111) | SO_4^{2-} aqueous solution interface the formation of the compact adsorption phase (layer) is possible, but comparatively slow process [1]. The so-called frequency dispersion discussed by Hamelin [7] has been explained later by low adsorption rates of specifically adsorbed anions on Au (*hkl*) [1,8]. For Ag(111) electrode the adsorption of Cl^- ions starts near –0.7 V (vs. sat. calomel electrode, SCE) while adsorption of Br^- ions starts at $E =$ –1.0 V (SCE). A disordered adlayer is formed up to potential of –0.1 V and an ordered adlayer for the anions as an unrotated (1.38×1.38) structure and $(\sqrt{3} \times \sqrt{3})$ R 30^0 adlayer for Br^- ions has been observed, using ex situ reflection energy electron diffraction and in situ STM methods [10–17]. At electrode potentials more positive than the potential of sharp capacitance peak in the capacitance vs potential curves or the current density peak in the current density vs. potential curves, the more compressed adsorption overlayer structure has been observed [16,17]. However, the sum of the double layer and adsorption capacitances (independent of ac frequency) could be obtained only at very low frequency ($f <$ 2 Hz) [2]. For real polycrystallic surfaces the situation is more complicated [2].

The strong adsorption of iodide and chloride ions was detected on Bi single crystal planes from aqueous and non-aqueous supporting electrolyte solutions [5,6,31–34]. Analysis of the impedance data can help to understand the complicated adsorption behavior of iodide ions at the Bi(*hkl*) planes within a wide potential region. The impedance data of I^- and Cl^- can be fitted with classical Frumkin−Melik-Gaikazyan (FMG) model.

The thermodynamics of the halides adsorption has been discussed and analyzed in detail by Parsons [18], Lipkowski et al.[19,20], Schmickler [21], Damaskin et al. [24–26], Vorotyntsev and Golub [27,28], as well as by Schultze and Vetter [29], Scmickler and Guidelli [30]. There are some differences in the thermodynamic data obtained using various measurement methods and it is probably mainly caused by the slow adsorption rate of the halide anions as well as by the partial charge transfer process from the adsorbed halide ions to the metal surface depending on the chemical nature of the electrolyte studied [19–21,29–33]. For example, Lipkowski et al. [19] observed that the charge densities calculated by using differential capacitance, chronocoulometry and voltammetry methods differ each other even if the same method has been used for the surface preparation of the Au(*hkl*) electrode.

4.2 Ionic liquids

4.2.1 Physical properties of ionic liquids [35–36]

An ionic liquid (IL) is a salt in the liquid state, that consists of large organic cations and smaller inorganic anions or vice versa. Ionic liquids are usually liquid below 100 °C.

4.2.1.1 Viscosity

Ionic liquids are more viscous than common molecular solvents and high viscosity is determined by van der Waals forces and hydrogen bonding. Electrostatic forces may also play an important role. Viscosity of IL increases with the increase of alkyl chain's length because of stronger van der Waals forces between cations. Hydrogen bonding between anions also accrues viscosity.

4.2.1.2 Conductivity

Ionic liquids have relatively good ionic conductivity, based on the fact that they consist only of ions, but at room temperatures their conductivities are lower than in concentrated aqueous electrolyte solutions. Conductivity depends not only on the number of charge carriers but also on their mobility, it indicates that ionic liquids that consist of large ions have lower conductivity. Ionic liquids with higher viscosity leads to lower conductivity. Increase in temperature lowers viscosity and increases conductivity.

4.2.1.3 Density

Ionic liquids are denser than water with density from 1 to 1.6 g cm^{-3} and their densities decrease with increase in the length of the alkyl chain in the cation. Density of ionic liquids is also affected by identity of anions.

4.2.1.4 Melting point

Ionic liquids have low melting point below 100 °C and most of them are liquid at room temperature. Both anion and cation structures play an important role in low melting point of IL. If anion size increases, the melting point decreases and if cations are large and asymmetrically substituted, it reducts melting point.

4.2.1.5 Thermal stability

Ionic liquids are known for their good thermal stability up to 450 °C. The thermal stability of ionic liquids is limited by the strength of their heteroatom–carbon and heteroatom–hydrogen bonds, but ionic liquids can tolerate such high temperature only for short time, otherwise they decompose.

4.2.1.6 Electrochemical window

The role of the region of ideal polarizability, i.e. electrochemical window is significant using ionic liquids in electrochemical measurements (electrodeposition of metals, semiconductors and supercapacitors). Electrochemical stability of solvents and electrolytes determine the electrochemical window. The electrodeposition of elements and compounds from aqueous electrolyte solutions is limited by low electrochemical window, but in ionic liquids it is noticeable wider.

4.2.2 Ionic liquids in electrochemistry

Recent research activity of ionic liquids, initiated by their potential applications in various modern electrochemical power systems, created interest in the interface between ionic liquids and metal [37–49] as well as carbon, including nanoporous carbon electrodes [50–52]. They are increasingly being used in applications such as green synthesis [54,55], catalysis with transition metals [56,57], and in electrochemical applications such as electrodeposition of metals [58], as electrolytes in lithium-ion batteries [59–61], sensors [62–66], supercapacitors [67–69], solar cells [70], and fuel cells [71].

RTILs are currently being investigated as possible electrolytes for gas sensing applications [55], since their favorable properties (low-volatility and high thermal stability) means that the sensor does not dry out, and provides the possibility for gas sensing at high temperatures, which may be of use in the combustion industry and elsewhere. Potentiometry with ion selective electrodes (ISEs) is an accurate, fast, and inexpensive analytical method [63–66]. ISEs have provided the possibility to detect chemical species with reasonable selectivity and low detection limit. ILs were found to be excellent materials to prepare membranes for ISEs due to their polymer plasticizing ability and ionic nature.

Electrochemical capacitors, based on the differential capacitance of the double layer formed at the carbon/electrolyte interface, have received considerable attention as they can be used as high power density energy storage devices. Both carbon materials as well as electrolytes have been developed for application in various systems. Many aqueous and organic liquid solutions of electrolytes have been used in electrochemical capacitors. Because of the superior properties of ionic liquids they have recently widely been studied as electrolytes in EDLC [67–69].

Ionic liquids have been used in lithium-ion batteries as novel candidates for electrolyte solvents [59–61]. $EMImBF_4$ (1-ethyl-3-methyl imidazolium) series RTILs have been widely used for battery applications since the discovery of $EMImBF_4$ because of their moderate viscosity and conductivity. Among many from the series of RTILs, quaternary ammonium cation-imide combinations are fairly interesting because of their higher electrochemical stability especially in the reduction reaction, but in this case graphitized carbon materials for Li-ion batteries have difficulty in obtaining the practical Li+ intercalation/deintercalation capacitance without additives. RTILs improve the safety of Li-ion batteries with carbon negative electrodes. To date, RTILs are the most promising electrolytes for improving the safety of Li-metal batteries which could be important for higher energy densities, i.e. for transportation applications.

Ionic liquids are good solvents for catalytic reactions [56–57]. The rational selection of the appropriate ionic liquid solvent for a particular reaction requires general knowledge about the properties of ionic liquids, and the details of some properties of the specific ionic liquid solvents being considered.

A fuel cell is an electrochemical device that converts a fuel into an electrical current. Fuel cells are made up of three segments: the anode, the electrolyte and the cathode. Brønsted acid-base ionic liquids, inorganic and organic ionic liquids have been investigated as the electrolyte candidates for fuel cells electrolytes [72–74]. Inorganic ammonium salt mixtures can actually be used in place of the commonly used organic ionic liquids as fuel cell electrolytes. The fuel cell electrodes can operate in the same temperature range as existing fuel cells, while the efficiencies at low current densities can be much better [75].

4.3 Electrochemical impedance spectroscopy

Electrochemical impedance spectroscopy (EIS) method is based on the system response to the application of a periodic small amplitude ac signal, and therefore these measurements are carried out at different ac frequencies. Analysis of the system response contains information about the interface, its structure and reactions taking place at the interfaces.

System impedance is a complex parameter and may be represented in Cartesian form as,

$$Z = Z' + \mathrm{j}Z'' \qquad [4.3.1]$$

where the real and imaginary parts of the impedance are: $Z' = R$ and $Z'' = -1/\omega C$, respectively.

$$\delta = \arctan \frac{|Z''|}{Z'} \qquad [4.3.2]$$

δ is the phase-angle between the ac current and potential applied. The current has the same frequency as the applied potential but can be phase-shifted by the angle δ depending on the system characteristics.

On ideally polarizable solid electrodes the electrical equivalent model can be usually represented (including the monocrystalline electrodes in the case of absent adsorption) as a series connection of the solution resistance and double-layer capacitance. However, on solid electrodes frequency dispersion is observed, that is the observed impedances cannot be represented by connection of simple R-C elements. The impedances may often be represented by an equation without simple electrical representation, i.e. through the so-called distributed elements. The Warburg impedance is an example of a distributed element.

Experimental impedance data in this work were fitted by using the equivalent circuits shown in Fig. 1, where R_{el} is the high-frequency series resistance equal to the electrolyte solution resistance at $f \rightarrow \infty$; C_{dl} is the so-called “true” high-frequency differential double layer capacitance, obtained at $f \rightarrow \infty$ ($C_{\mathrm{dl}} = (\partial q/\partial E)_{\Gamma,\mu}$, where q is the electrode charge density, Γ is the Gibbs adsorption and μ is the chemical potential); adsorption capacitance C_{ad} is equal to $(C_0 - C_{\mathrm{dl}}) = (\partial q/\partial \Gamma)_E\, (\partial \Gamma/\partial E)_\mu$, where thermodynamic low-frequency capacitance $C_0 = (\partial q/\partial E)_{\Gamma,\mu} + (\partial q/\partial \Gamma)_E\, (\partial \Gamma/\partial E)_\mu$ is obtained at $f \rightarrow 0$; $Z_{\mathrm{w}} = \sigma_{\mathrm{ad}}(\mathrm{j}\,\omega)^{-1/2}$ is Warburg-like diffusion impedance ($\sigma_{\mathrm{ad}} = \tau_{\mathrm{D}}^{1/2} C_{\mathrm{ad}}^{-1}$ is the Warburg constant, where τ_{D} is the diffusion relaxation time); CPE is the constant phase element and the CPE impedance Z_{CPE} is equal to $A^{-1}(\mathrm{j}\,\omega)^{-\alpha}$ (A is a CPE constant and α is fractional exponent; if $\alpha = 1$ then $A = C_{\mathrm{dl}}$); R_{ad} is the adsorption (or partial charge transfer) resistance ($R_{\mathrm{ad}} = \tau_{\mathrm{H}} C_{\mathrm{ad}}^{-1}$, where τ_{H} is adsorption relaxation time); and R_{p} is the parallel resistance, calculated according to the classical conception discussed in elsewhere [76-80]. The goodness of a fit is estimated by the value of the χ^2 – function, weighted sum of squares (Δ^2), and by the relative errors of each parameter in the equivalent circuit (EC) under analysis.

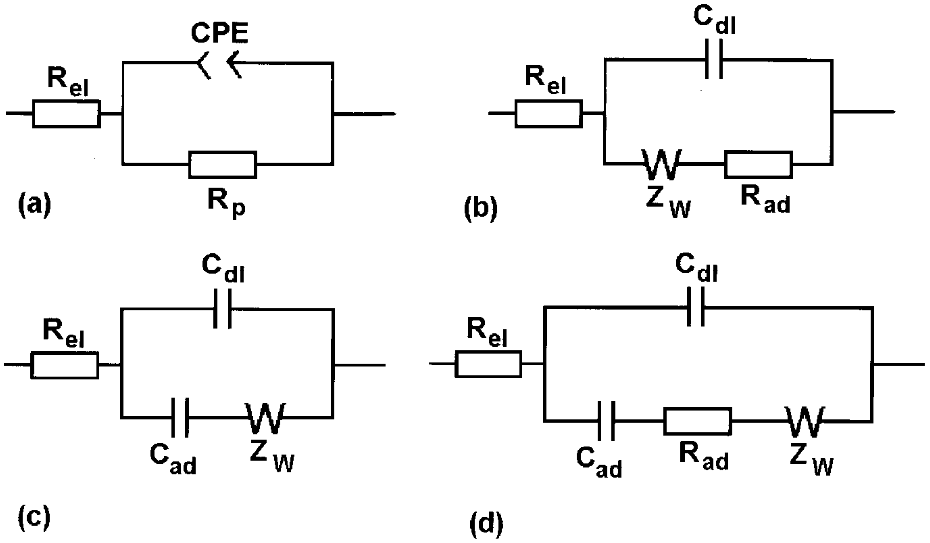

Fig. 1. Equivalent circuits used for fitting the experimental data. R_{el} is the electrolyte solution (high frequency) resistance, C_{dl} is the double layer capacitance at ac $f \to \infty$, C_{ad} is the adsorption capacitance, Z_w is the Warburg-like diffusion impedance defined as $Z_W = \sigma_{ad}(j\omega)^{-1/2}$, where σ_{ad} is the coefficient of the Warburg impedance. CPE is the constant phase element with impedance $Z_{CPE} = A^{-1}(j\omega)^{-\alpha}$ (A is a constant and α is a fractional exponent, CPE = C_{dl} if α=1). R_{ad} is the adsorption or partial charge transfer resistance and R_p is the parallel charge transfer resistance.

4.4 Cyclic voltammetry

Cyclic voltammetry is the most widely used technique for acquiring qualitative information about electrochemical reactions. In a typical cyclic voltammetry method, a solution component is electrolyzed (oxidized or reduced) by placing the solution in contact with an electrode surface, and then making that surface sufficiently positive or negative in voltage to initiate the electron transfer. It enables the electrode potential to be rapidly scanned in search of redox couples. Once located, a couple can then be characterized from the potentials of peaks on the cyclic voltammogram and from current changes caused by variation of the potential scan rate. CV analysis is often the first experiment or method performed in an electrochemical study. To obtain a cyclic voltammogram, the current at the working electrode is measured during the potential scan.

Usually the electrode potential is ramped linearly to a more negative potential, and then ramped in reverse back to the starting voltage. The forward scan produces a current peak for any analytes that can be reduced through the range of the potential scan. The current will increase as the potential reaches the reduction potential of the analyte, but then falls off as the concentration of the analyte is depleted close to the electrode surface. As the applied potential is reversed, it will reach a potential that will reoxidize the product formed in the first reduction reaction, and produce a current of reverse polarity from the forward scan. This oxidation peak will usually have a similar shape to the reduction peak. The peak current, i_p, is described by the Randles-Sevcik equation:

$$i_p = (2.69\text{x}10^5)\, n^{3/2}\, \mathrm{A}\, c\, D^{1/2}\, v^{1/2} \qquad [4.4.1]$$

where n is the number of moles of electrons transferred in the reaction, A is the area of the electrode, c is the analyte concentration (in moles/cm^3), D is the diffusion coefficient, and v is the scan rate of the applied potential.

5. EXPERIMENTAL

5.1 Measurements in aqueous solutions

The adsorption kinetics of iodide ions at electrochemically polished Bi(001) and Bi(111) single crystal planes from aqueous solutions with constant ionic strength $0.1x$ M KI+$0.1(1\text{-}x)$ M KF and $0.1x$ M KI+$0.033(1\text{-}x)$ M K_2SO_4 was studied by ac impedance spectroscopy (0.1 stands for the total concentration of solution and x is the mole fraction of KI in a solution). Measurements were carried out in the solutions with constant ionic strength to minimize the influence of the changes in the total solution concentration on the diffusion and adsorption steps. Solutions were prepared from KF, KI and K_2SO_4 (Aldrich Chemical Company, 99.998%) and Milli Q+ water (ultra purified water using the Milli Q+ purification system, resistance > 18.2 MΩ cm). Surface preparation of the electrodes was carried out before each experiment by electrochemical polishing in an aqueous solution of KI+HCl. After that the electrodes were rinsed carefully with Milli Q+ water and polarized at –1.2 V (vs. Ag | AgCl | 4M KCl aqueous solution) in surface- inactive electrolyte solution, which was previously saturated with the electrolytic hydrogen for minimum 2 hours. The quality of the Bi single crystal electrodes were tested by X-ray diffraction, in situ STM, AFM and ultra high vacuum STM methods. The experimental impedance spectra were measured using Autolab PGSTAT 30 FRA 2 ($0.1<f<10000$ Hz, 100 different frequencies).

5.2 Measurements in ionic liquids

Bi(111)|ionic liquid (1-ethyl-3-methylimidazolium tetrafluoroborate ($EMImBF_4$), >99.0%, ≤ 200 ppm H_2O, Fluka; 1-ethyl-3-methylimidazolium tris(pentafluoroethyl)trifluoro-phosphate (EMImFAP), 99.9%, ≤ 100 ppm H_2O, Merck KGaA and 1-ethyl-3-methylimidazolium tetracyanoborate (EMImTCB), 99.9%, ≤ 100 ppm H_2O, Merck KGaA) interface has been studied by cyclic voltammetry (CV) (potential cyclation rate was varied from 0.5 to 500 mV s^{-1}) and impedance spectroscopy ($0.1<f<10000$ Hz, 100 different frequencies) using Autolab PGSTAT 30 FRA 2 at temperature 296±0.1 K inside glove box (Labmaster sp, LMBraun; O_2 and H_20 concentrations <0.1 ppm). The Bi(111) electrode was electrochemically polished before each experiment in the KI+HCl aqueous solution. After polishing the electrode was rinsed with Milli Q+ water, dried by Ar (99.99995%) and by ionic liquid. Ionic liquids were saturated for 24 hours with Ar (99.99995%) before submerging the electrochemically polished Bi (111) electrode into electrolyte. Electrochemically stable current densities have been established after at least 2 hours polarization of the electrode at –0.7 V (vs. Ag | AgCl | ionic liquid currently measured).

6. RESULTS AND DISCUSSION

6.1 Adsorption of iodide ions at Bi(111) and Bi(001) single crystal electrodes

[I, II]

Cyclic voltammetry and electrochemical impedance spectroscopy have been applied for investigation of adsorption kinetics of iodide ions from aqueous electrolyte solutions at electrochemically polished Bi(*hkl*) electrodes. The cyclic voltammetry (*j* vs. *E*) curves show that the Bi(111) electrode is ideally polarizable within the regions of $-1.4 < E$ -0.55 V (vs. Ag|AgCl|4M KCl) in the aqueous solution with constant ionic strength 0.1x M KI+0.033(1-x) M K_2SO_4 and Bi(001) is ideally polarizable within the potential region from –1.4 V to –0.5 V (vs. Ag|AgCl|4M KCl) in the aqueous solution of 0.1x M KI + 0.1(1-x) M KF. The electrochemical impedance spectroscopy method has been used for the quantitative study of I^- ions adsorption at bismuth single crystal planes.

The complex impedance plane -*Z'', Z'* – plots, i.e. Nyquist plots, where *Z''* is an imaginary component ($Z'' = -\frac{1}{C_s\omega}$, C_s is the total series capacitance at fixed angular frequency $\omega = 2\pi f$, where f is ac frequency), and *Z'* is a real part of the impedance [76–85] at different electrode potentials and mole fractions of KI, are shown in Figs. 2 and 3, where points are experimental data and solid lines are fitting results (discussed later). The shape of a *Z'', Z'* curve depends noticeably on the electrode potential applied (Fig. 2) and on the amount of the surface active electrolyte KI in the solution (Fig. 3). At fixed KI concentration, c_{KI}, and *Z'*, the absolute value of Z'' slightly decreases with the decrease of negative potential of the electrode from –1.2 to –0.5 V (vs. Ag|AgCl|4M KCl), which is explained by the weak adsorption and partial charge transfer from the adsorbed I^- anions to the Bi(001) and Bi(111) surface [23, 31–33, 76,77].

In the region of intensive increase of the differential capacitance C_s ($-0.7 < E \leq -0.5$ V) the impedance spectra for Bi(*hkl*) have a complicated shape (Fig. 2) and can be fitted by tilted non-linear curves rather than by the semicircles, characteristic of the true faradic process [76–85]. In this region of electrode potentials, the value of $|Z''|$ increases with increasing the mole fraction of KI in the solution (Fig. 3) because of the noticeable adsorption and partial charge transfer process. In the region of more negative potentials than –1.4 V the slight increase in the current density can be observed and the impedance spectra become a shape of slightly depressed semicircles, which indicate the beginning of the faradic process (hydrogen evolution from KF +KI aqueous solutions) or can be explained by the slow adsorption of K^+ ions following by the partial charge transfer process. These parts of the -*Z''*,*Z'* spectra have not analyzed in detail in this work.

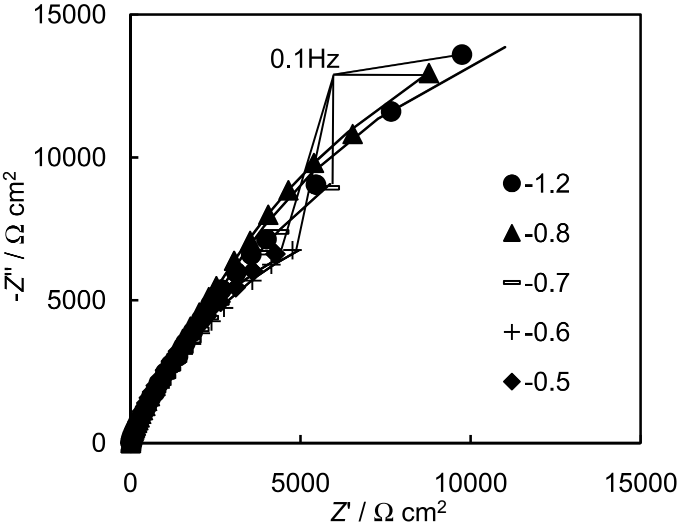

Fig. 2. Complex impedance plane plots for the Bi(001) electrode in 0.1 M KI aqueous solution at different electrode potentials *E* (V vs. Ag | AgCl), noted in figure. Marks – experimental data, and solid lines – fitting according to the Frumkin-Melik-Gaikazyan equivalent circuit (c in Fig. 1).

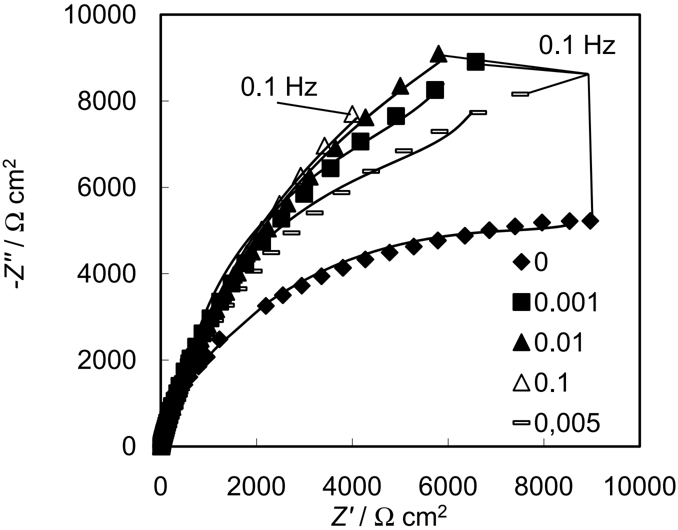

Fig. 3. Complex impedance plane plots for the Bi(001) electrode at –0.5 V in 0.1*x* M KI + 0.1(1-*x*) M KF aqueous solutions at different mole fractions of KI, *x* (M), noted in figure. Marks – experimental data, and solid lines – fitting according to the FMG equivalent circuit (c in Fig. 1).

The dependence of the phase angle δ ($\delta = \arctan(|Z''|/Z')$) on log f is presented in Figs. 4, because the *Z*'',*Z*' plots do not indicate the all needful information. Differently from the non-aqueous LiI solution | Bi(*hkl*) interface the shape of the δ, log*f* curves is nearly independent of KI concentration if $E < -0.8$ V and $c_{\mathrm{KI}} < 0.05$M (Ag | AgCl) (Fig. 4 a).

In the low- frequency range from 0.1 to 1 Hz, δ values change from –58 to –60°, indicating the kinetically mixed process (i.e. the total rate of the process becomes limited by the rates of diffusion-like and adsorption steps as well as partial charge transfer). The high absolute values of $|\delta| \approx 80°$ obtained in the moderate ac frequency region from 10 to 100 Hz show that the adsorption of the solution components at Bi(001) and Bi(111) planes is limited mainly by the rate of adsorption step [5,6,78–83].

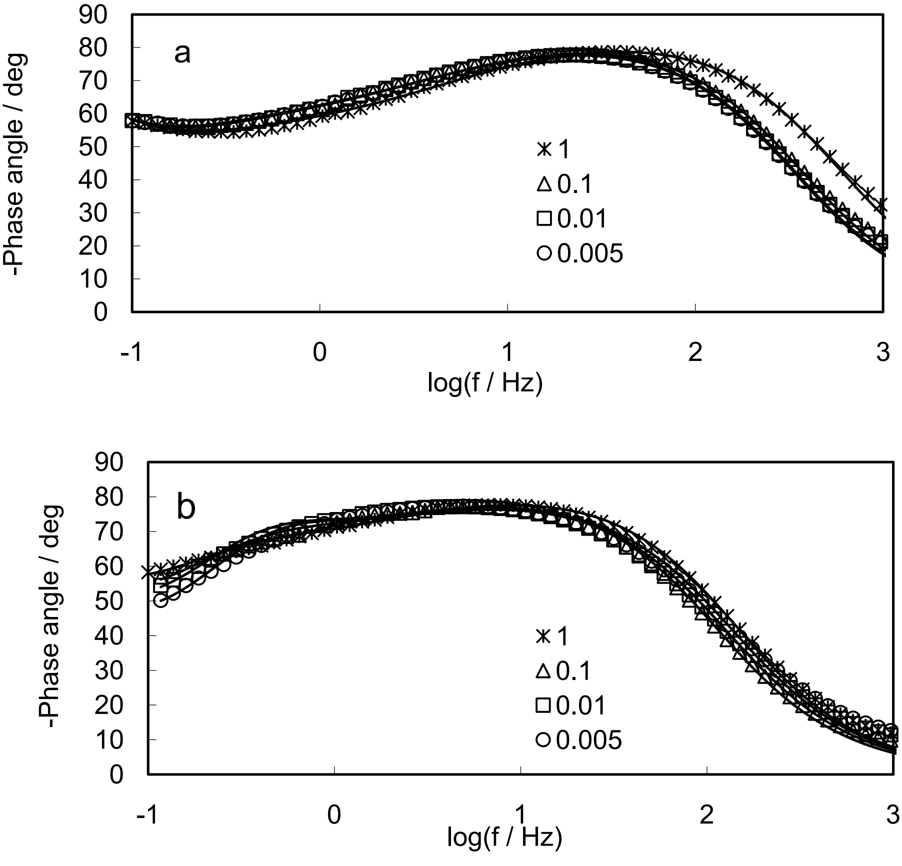

Fig. 4. Dependence of the phase angle (δ) on ac frequency for the Bi(111) electrode in $0.1x$ M KI + $0.033(1\text{-}x)$ M K_2SO_4 aqueous solutions at the various fixed electrode potentials –1.2 V (a), –0.5 V(b) at the mole fractions of KI, x (M), noted in figure.

In the region of less negative potentials ($E \geq -0.8$ V vs. Ag | AgCl | 4M KCl) there is a certain dependence of the phase angle on the concentration of KI at ac frequency $f < 1$ Hz as well as at $f > 10$ Hz. In ac frequency range from 1 Hz to 10 Hz the experimental data show that the main limiting stage is the adsorption step $|\delta| > 75^o$(Fig. 4b). In the high- frequency range $f > 1\,00$ Hz the absolute values of phase angle increase with c_{KI}, indicating the rise of the role of the adsorption step in the adsorption kinetics, but the limiting stage is still mixed kinetics (diffusion, adsorption and partial charge transfer) with $|\delta| > 45^{\circ}$. Thus, in the potential region of intensive adsorption of the I^- ions (near –0.5 V vs. Ag | AgCl) (Fig. 4b), there is a considerable dependence of δ on the concentration of KI, the limiting stage is the mixed kinetic step (slow adsorption, diffusion as well as partial charge transfer steps, discussed in [31–33]). At $f < 1$ Hz the absolute values of phase angle $|\delta|$ decrease from 50° to 60°, hence, they are closer to $|\delta| = 45°$, which is characteristic of the semi- infinite diffusion step limited processes [76–85]. A noticeable dependence of the phase angle on c_{KI} in the region of ac frequency from 100 Hz to 1000 Hz indicates the dependence of the inner layer structure of the electrical double layer on c_{KI}. In the high ac frequency region there is no dependence of $|\delta|$ on the electrode potential in the case of 0.1 M KF as it was established for $LiClO_4$ solutions in ethanol [5] as well as for KI containing solutions in this work, which indicates that, contrary to the weakly solvated ClO_4^- and I^- ions in ethanol [5,6] and I^- in water, the F^- ions are unable to enter into the inner part of the electrical double layer. Thus, the solvated F^- ions are practically surface inactive at the Bi(001) | aqueous solution interface. The same is valid for the K_2SO_4 aqueous solution as base electrolyte (Fig 4b).

6.1.1 Analysis of impedance data

The theoretical impedance data were calculated based on the equivalent circuits shown in Fig. 1 using the non-linear least squares fitting with the experimental impedance data. The best fitting results were obtained with the modified Frumkin-Melik-Gaikazyan equivalent circuit (FMG EC) (circuit c in Fig. 1). The results of fitting show that the values of the fractional exponent, α_W, for the Warburg like diffusion impedance are close to 0.5 (Fig. 5), demonstrating that the deviation of Bi(111)|KI+H_2O interface from the traditional semi-infinite diffusion model is weak [76–80, 84,85].

According to the data measured at Bi(001), the electrolyte resistance R_{el} (fitting error $\approx$1%) is independent of electrode potential (Fig. 6a), but there is a weak dependence of R_{el} on the concentration of the surface active component (KI) because the molar conductivity of KI is somewhat higher than that for KF.

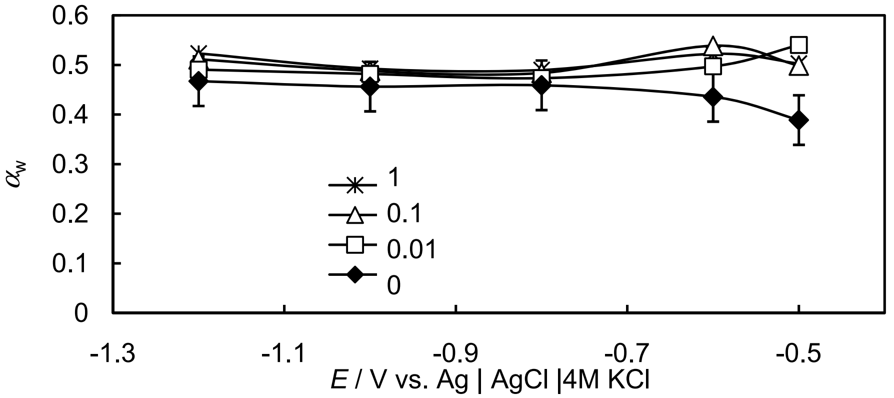

Fig. 5. Dependence of fractional exponent α_W on the electrode potential for Bi(001) in 0.1*x* M KI + 0.1(1-*x*) M KF aqueous solutions at various mole fractions of KI, *x* (M), noted in figure. Statistical error bars obtained using five independent experiments are given in figure.

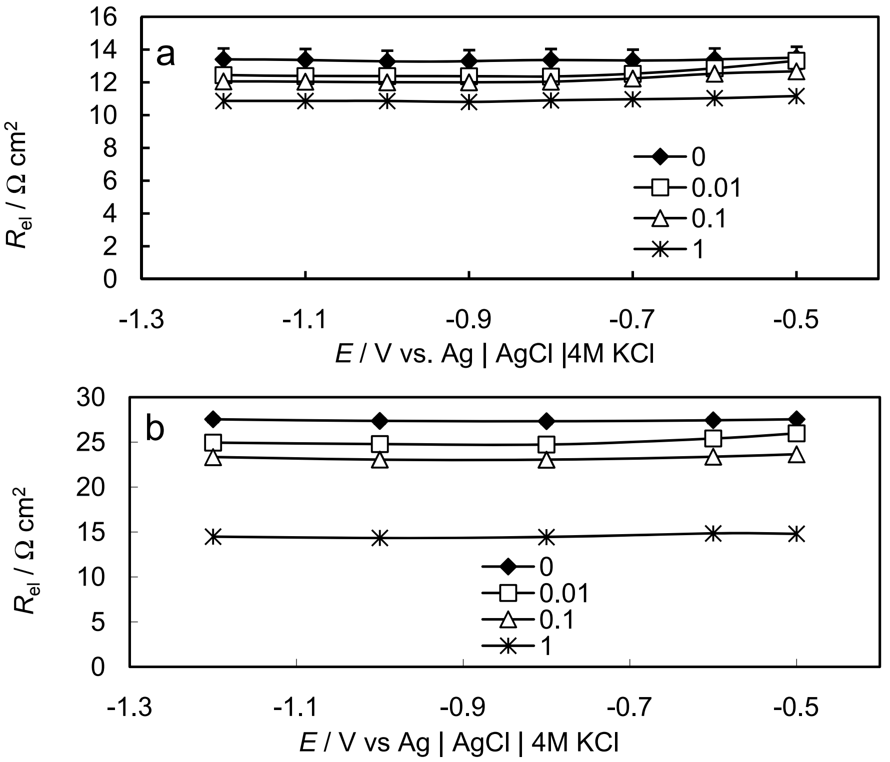

Fig. 6. Dependence of the electrolyte resistance R_{el} on the electrode potential for Bi(001) in 0.1*x* M KI + 0.1(1-*x*) M KF (a) and for Bi(111) in 0.1*x* M KI + 0.033(1-*x*) M K_2SO_4 (b) aqueous solutions at various mole fractions of KI, *x* (M), noted in figure. Statistical error bars obtained using five independent experiments are given in figure.

It is caused by fact that the I^- ions are less solvated than F^- ions and the resistance of the electrolyte solution decreases with increasing c_{KI} in the mixed electrolyte solution. In Fig. 6b it can be seen that for Bi(111)|K_2SO_4 electrolyte interface as for surface inactive electrolyte there is no dependence of R_{el} on electrode potential.

The 'true' double layer capacitance (Fig. 7), C_{dl}, considerably depends on the concentration of KI in the potential range from –1.0 to –0.5 V (vs. Ag | AgCl) and C_{dl} increases with $c_{KI.}$ It can be explained with the specific adsorption of I^- at the Bi(001) and Bi(111) electrode surfaces at less negative electrode potentials [23, 31–33]. The dependence of C_{dl} on the mole fraction of KI indicates that the inner layer structure depends on the values of Gibbs adsorption Γ of the I^- ions.

The values of C_{ad}, adsorption capacitance, indicate that the adsorption process of I^- ions takes place at Bi(*hkl*) electrodes. The values of C_{ad} show some expansion in both ends of the region of ideal polarizability (Fig. 8). At $E > –0.7$ V, the weak increase in the values of C_{ad} with increasing c_{KI} has been observed, which can be explained by the intensive specific adsorption of iodide ions at the Bi(*hkl*) electrode surface. However, there is no noticeable dependence of C_{ad} on c_{KI} at $E < –1.2$ V where the adsorption of I^- ions is negligible.

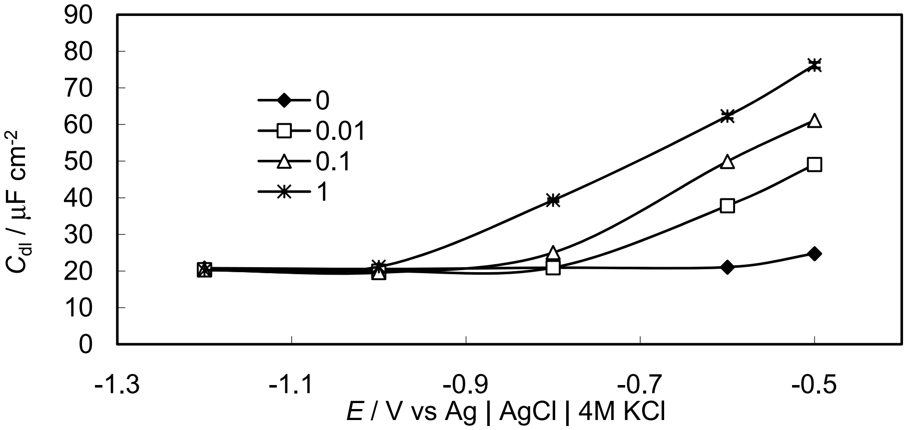

Fig. 7. Dependence of 'true' double layer capacitance C_{dl} on the electrode potential for Bi(111) in 0.1*x* M KI + 0.033(1-*x*) M K_2SO_4 aqueous solutions at various mole fractions of KI, *x* (M), noted in figure. Statistical error bars obtained using five independent experiments are given in figure.

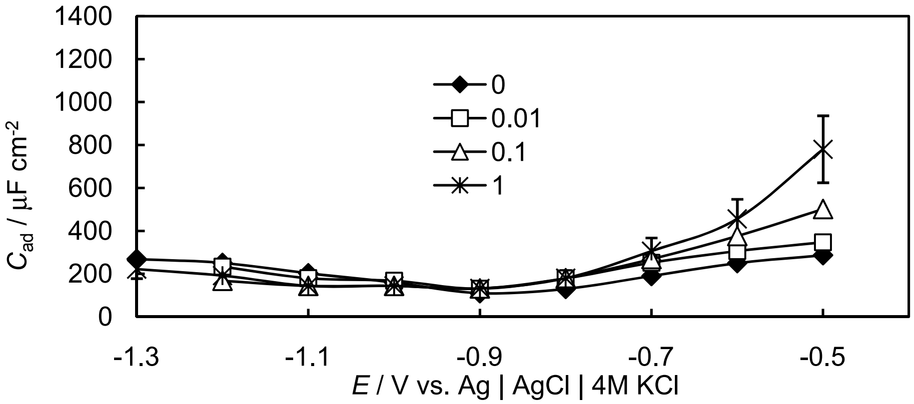

Fig. 8. Dependence of adsorption capacitance C_{ad} on the electrode potential for Bi(001) in 0.1x M KI + 0.1(1-x) M KF aqueous solutions at various mole fractions of KI, x (M), noted in figure. Statistical error bars obtained using five independent experiments are given in figure.

The diffusion resistance R_D has maximum values in the region of potentials (Fig. 9.), where the specific adsorption of I^- ions at Bi(hkl) starts, i.e. in the region of intensive increase of the differential capacitance in the C,E curves. The same effect has been established for Bi(hkl) | non-aqueous surface active electrolyte systems (LiI) [31–33]. The decrease in R_D at $E > -0.9$ V can be explained by the specific adsorption of the I^- ions [5,6, 31–33]. Taking into account the relative error obtained from various experiments as well as fitting errors, there is no clear dependence of R_D on the concentration of KI. The so-called mass transfer frequency factor (T) also depends on the electrode potential and somewhat increases with c_{KI} at $E > -0.7$ V (Fig. 10).

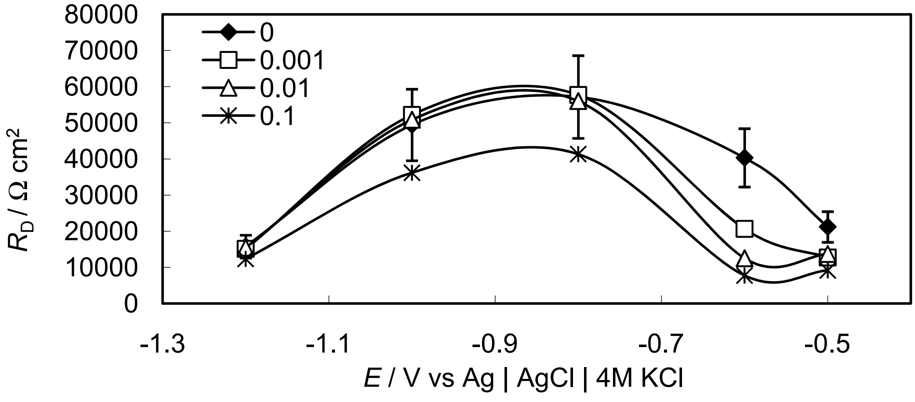

Fig. 9. Dependence of diffusion resistance R_D on the electrode potential for Bi(111) in 0.1x M KI + 0.033(1-x) M K_2SO_4 aqueous solutions at various mole fractions of KI, x (M), noted in figure. Statistical error bars obtained using five independent experiments are given in figure.

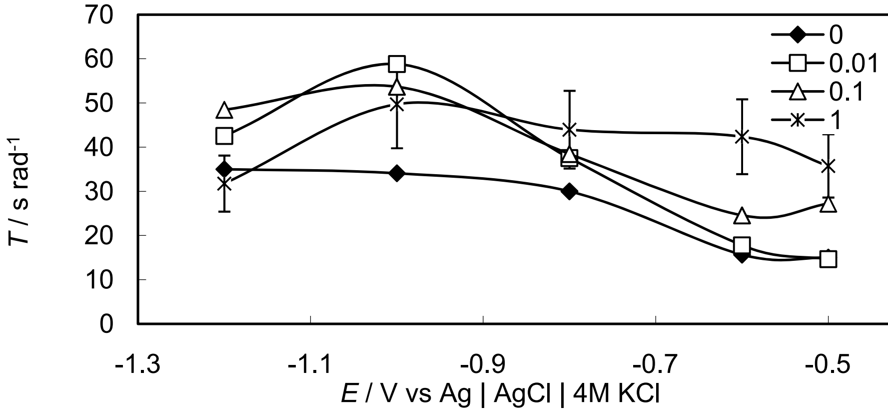

Fig. 10. Dependence of mass transfer frequency factor (*T*) on the electrode potential for Bi(001) in 0.1*x* M KI + 0.1(1-*x*) M KF aqueous solutions at various mole fractions of KI, *x* (M), noted in figure. Statistical error bars obtained using five independent experiments are given in figure.

For conclusion the electrical double layer capacitance, adsorption capacitance, diffusion resistance and other adsorption characteristics depend on the electrode potential applied. However, there is no noticeable dependency of these parameters on the mole fraction of the surface active I^- anion in the electrolyte solution at moderate negative potentials (i.e. in the region where there is no specific adsorption of anions). At $E > -1.0$ V for Bi(111) and Bi(001), there is a noticeable dependence of C_{ad} and C_{dl} on the mole fraction of KI, thus, if the intensive specific adsorption of the I^- ions starts. Analysis of complex impedance plane and phase angle vs. ac frequency curves shows that adsorption of I^- anions is limited by mixed kinetics (slow adsorption and diffusion-like steps), but the rate of adsorption step is limiting at moderate frequencies.

6.2 Properties of electrical double layer at Bi(111)|ionic liquid interface [III–V]

Cyclic voltammetry and electrochemical impedance spectroscopy have been applied for investigation of the electrochemically polished Bi(111) electrode in 1-ethyl-3-methyl imidazolium tris(pentafluoroethyl)trifluorophosphate (EMImFAP), 1-ethyl-3-methyl imidazolium tetracyanoborate (EMImTCB) and 1-ethyl-3-methyl imidazolium tetrafluoroborate ($EMImBF_4$) ionic liquids. These RTILs were chosen to investigate the influence of the chemical composition, structure and possible dependence of the closest approach of ions, i.e. specific adsorption of the ionic liquid anions on the electrical double layer capacitance (well-known for halide, CN^- and SCN^- ions from the aqueous and non-aqueous electrolytes).

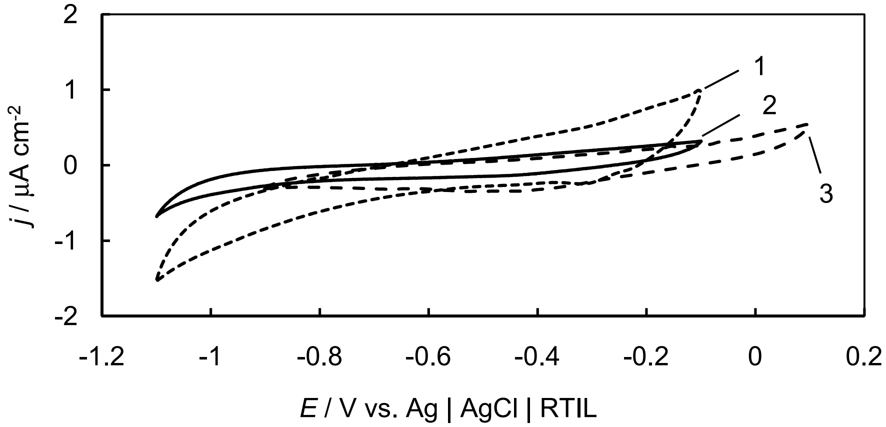

Fig. 11. Cyclic voltammograms for Bi(111) in EMImTCB (1); $EMImBF_4$ (2) and EMImFAP (3) at potential scan rate 10 mVs^{-1}.

Analysis of current density (j) vs. electrode potential (E) dependences (Fig. 11) show that the Bi(111) electrode is ideally polarizable (current density lower than 10^{-6} A cm^{-2}) from –0.9 to 0.1 V in EMImFAP and from –1.1 to 0.0 V in $EMImBF_4$ and EMImTCB. The increase in j outside these potential regions is caused by the faradic reduction and oxidation of residual water and oxygen as well as BF_4^- anions. At small negative or positive electrode potentials an anodic oxidation of metal takes place.

The width of the ideal polarizability region is in a good correlation with the data in impedance plane plots (Nyquist plots) — for Bi(111)|$EMImBF_4$ interface there are only weak deviations from the adsorption limited process mechanism within the region of $-0.9 < E < -0.2$ V (Fig.12a). For Bi(111)|EMImTCB and Bi(111)|EMImFAP, both adsorption and diffusion determine the rate of the total adsorption process similarly to the Bi(111)| $LiClO_4$ aqueous solution interface [86,87].

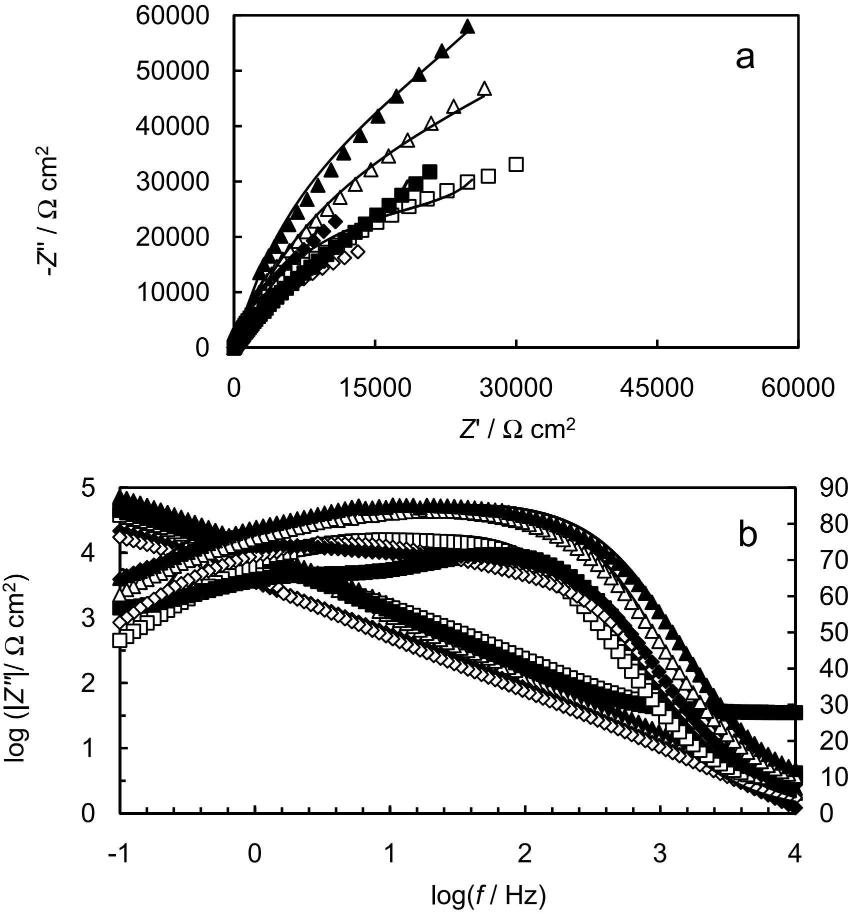

Fig. 12. Nyquist plots (a), impedance complex plane and phase angle plots (b) for Bi(111) in EMImBF$_4$ (triangles), EMImFAP (squares) and EMImTCB (rhombuses) at –0.7 (filled marks) and –0.1 V (open marks) (vs. Ag|AgCl|IL) (dots – exp. data, lines – fitting by Frumkin – Melik-Gaikazyan electrical circuit (EC) (c) in Fig.1).

Also the phase angle, δ ($|\delta| > 83°$ at $f < 10^2$ Hz) (Fig. 12b) and impedance modulus ($|Z|$) vs. frequency dependences for Bi(111)|EMImBF$_4$ confirm these conclusions. Only at very low ac frequency the small decrease in the negative values of phase angle has been established, which could be explained by occurring of the very slow first layer reorganization process of edl or partial charge transfer from ions to the electrode surface [88–90].

The experimental total series differential capacitance C_s (Fig. 13) has been calculated from the Nyquist dependences presented in Fig. 12a. The potential of the slight minimum in the constructed C_s vs. E plots, E_{min}, being located at –0.7 V, has found to be independent of ac frequency. The values of C_s for EMImFAP at E_{min} are noticeably lower than those for EMImBF$_4$, and especially for EMImTCB, and C_s for EMImFAP at $E > E_{min}$ is even lower than at $E < E_{min}$.

The lower capacitance values for EMImFAP can be explained by the larger molar volume (bigger diameter) for FAP$^-$ compared with BF_4^- or TCB$^-$.

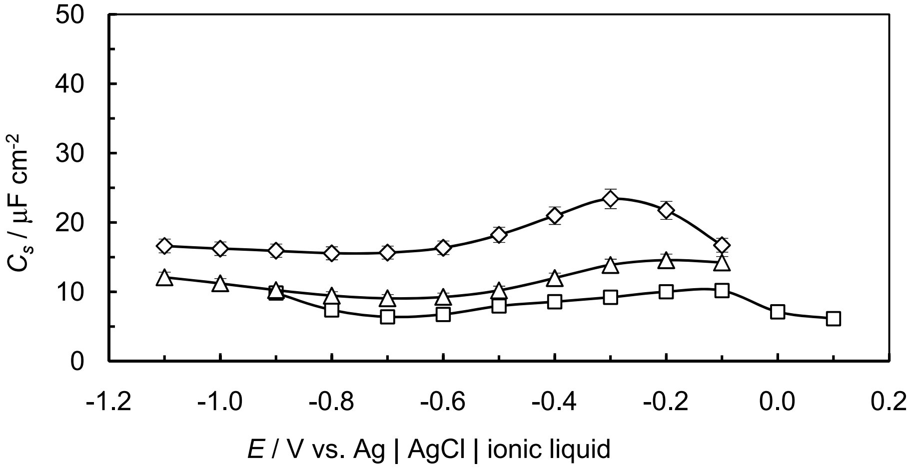

Fig. 13. Dependences of series capacitance vs. electrode potential curves for Bi(111)|$EMImBF_4$ (triangles), EMImFAP (squares) and EMImTCB (rhombuses) interface.

For Bi(111)|$EMImBF_4$ and EMImTCB (i.e. for RTILs with noticeable asymmetry of ions) the bell-shaped C_s,E curve has been found, but for EMImFAP (higher symmetry of molar volumes of ions) there is only a wide and low maximum at $E > E_{min}$. However, it seems that, in addition to the asymmetry of ions, the difference in surface activity, i.e. in the closest approach of anions to the electrode surface is also important, obtaining mainly the asymmetric shape of the inner layer capacitance vs. potential curve for BF_4^- and TCB$^-$ containing RTILs. The surface activity for EMImTCB seems to be noticeably higher than that for EMImFAP, explaining higher capacitance value for EMImTCB within the all potential region applied. Thus, the influence of second layer ions on C_s values, discussed by Kornyshev et al. [91–93] has been established. The same shape of “hump” in the C,E curve has been found to be characteristic of Hg in $LiBF_4$ or $LiClO_4$ and Bi(hkl) in $LiBF_4$, $LiClO_4$ and LiSCN aqueous and non-aqueous solutions [86,87].

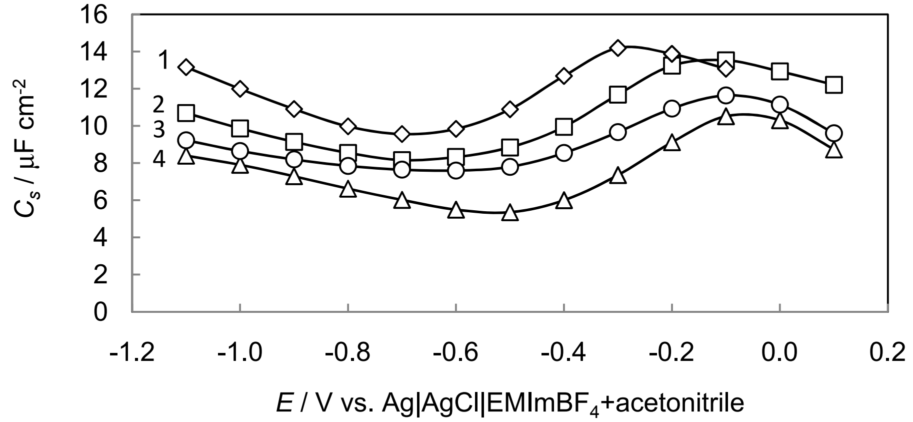

Fig. 14. Series capacitance vs. electrode potential curves for Bi(111)| x M EMImBF$_4$ + acetonitrile solution interface at 210 Hz and for x (M): 1 – pure; 2 – 0.5; 3 – 0.05; 4 – 0.005 EMImBF$_4$).

To analyze the influence of EMImBF$_4$ concentration on the capacitance and E_{min} values, the EMImBF$_4$ solutions in acetonitrile (H_2O < 0.003%, Riedel-de Haën) were studied using impedance method. For Bi(111)|acetonitrile (AN) + x M EMImBF$_4$ interface the decrease in series capacitance with dilution of the electrolyte has been observed and the well developed capacitance minimum has been established at $E = -0.5$ V vs. Ag|AgCl|EMImBF$_4$ in acetonitrile (Fig. 14). However, differently from LiClO$_4$ + AN solutions [86,87] the location of the minimum in the capacitance vs. potential curve for EMImBF$_4$ + AN solution depends strongly on the concentration of EMImBF$_4$ in acetonitrile. Thus, on the basis of Grahame electrical double layer model, the remarkable shift of E_{min} toward less negative potentials with the decrease of EMImBF$_4$ concentration indicates that the surface activity of BF_4^- anions is higher than that for EMIm$^+$ cations [86,87,89].

6.2.1 Simulation of impedance data

For calculation of the high-frequency double layer capacitance, C_{dl}, and equilibrium adsorption capacitance, C_{ad}, the equivalent circuit (EC) modeling method has been applied [85,88,89,94]. The non-linear least squares fitting shows that the more adequate fit of calculated with experimental spectra for Bi(111)|ionic liquid interface can be obtained by the modified Frumkin – Melik-Gaikazyan EC (Fig. 1(c)) where the classical semi-infinite diffusion impedance has been replaced by the open circuit finite length Warburg impedance $Z_{\mathrm{W(oc)}}$ [86,87,95–97]. Thus, the values of series capacitance (C_{s}) within the region of ideal polarizability can be divided into C_{dl} and C_{ad} (Fig. 15). Based on the fitting data, C_{dl} weakly depends of RTIL studied, corresponding to the edl structure, if there is no specific adsorption of anions with partial charge transfer [90] between the negatively charged electrode surface and RTIL anion. However, in the all potential region applied, C_{ad} is somewhat higher than C_{dl}, being higher for Bi(111)|EMImTCB compared with Bi(111)|EMImFAP interface, indicating the dependence of closest approach of anions onto the Bi(111) surface on the chemical structure of anions studied [13].

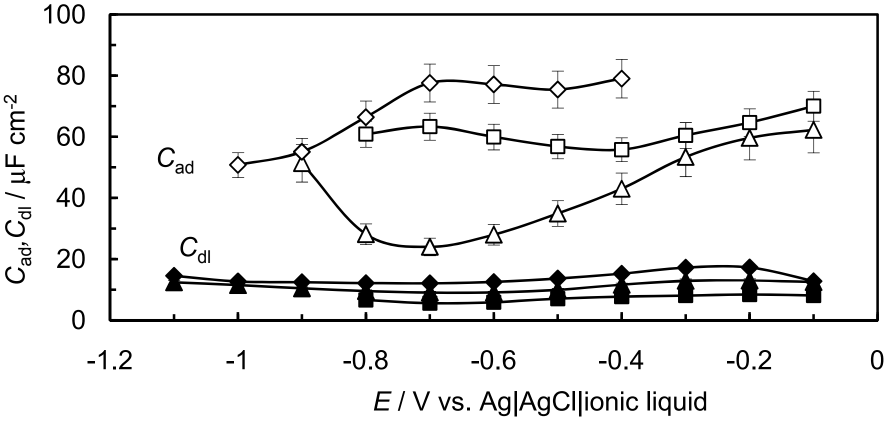

Fig. 15. Dependences adsorption capacitance C_{ad} and double layer capacitance C_{dl} vs. electrode potential curves for Bi(111) EMImBF$_4$ (triangles), EMImFAP (squares) and EMImTCB (rhombuses).

The diffusion-like process resistance R_D (Fig. 16) depends on RTIL studied, being higher for EMImBF$_4$. The values of fractional exponent of the Warburg-like diffusion impedance, α_W, are nearly 0.5 for EMImBF$_4$, thus the semi-infinite diffusion-like edl reorganization process takes place similarly to the Bi(111)|KF + KI aqueous solution interface (Fig. 16) [88]. Only for EMImTCB|Bi(111) interface the values of $\alpha_W > 0.5$ indicates the formation of ordered layer of adsorbate at the electrode surface.

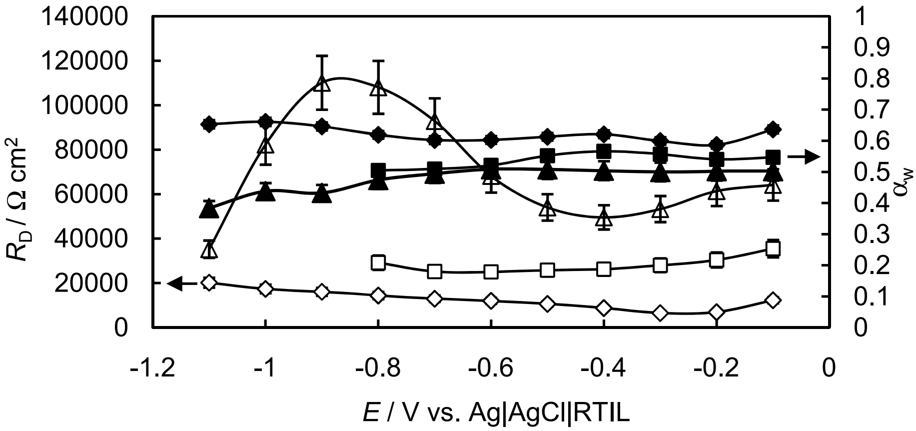

Fig. 16. Dependences of adsorption resistance R_D and fractional exponent in the generalized finite length Warburg impedance (α_W) on electrode potential for Bi(111) in EMImBF$_4$ (triangles), EMImFAP (squares) and EMImTCB (rhombuses).

For conclusion, cyclic voltammetry and impedance data show the strong dependence of electrical double layer capacitance, i.e. structure of Bi(111)|RTIL interface on the chemical composition, ion size asymmetry and surface activity.

6.3 Comparison of limiting stages of adsorption and some characteristic parameters of ionic liquids and aqueous solutions of KI at Bi(111) and Bi(001)

6.3.1 Analysis of limiting stages of adsorption

At cathodic potentials $E < -1.2$V (vs. Ag|AgCl|4M KCl) for systems Bi(001)|0.1x M KI+0.1(1-x) M KF; Bi(111)|0.1x M KI+0.033(1-x) M K_2SO_4 and at $E < -0.7$V (vs. Ag|AgCl|ionic liquid) (it should be noted that the potential difference between Ag|AgCl in 4M KCl+H_2O electrolyte and Ag|AgCl|RTIL reference electrodes is near –0.29V) for system Bi(111)|ionic liquid dependencies of the phase angle δ on log f plots are similar and a needful information of limiting stages of adsorption process can be expected. The shape of δ, log f curves is practically independent of KI concentration at both Bi electrodes measured. In the low-frequency range from 0.1 Hz to 1 Hz δ changes from -60° in aqueous solution of KI to -60–70° in ionic liquids, indicating that the kinetically mixed process (the total rate of process is limited by diffusion-like, adsorption and partial charge transfer steps) prevail at the Bi(hkl)|electrolyte interface. In the moderate ac frequency region from 10Hz to 100Hz δ, log f-curves demonstrate maximum values from -70° to -84° in ionic liquids and $\delta \cong$

-80° in aqueous solutions of KI indicating that the adsorption of solution components (i.e. ions) is mainly limited by the rate of adsorption step [5,6, 80–83].

At less negative potential, i.e. near to the end of ideal polarizability $E \geq -0.5$V (vs. Ag|AgCl|4M KCl) for systems Bi(001)|0.1x M KI+0.1(1-x) M KF; Bi(111)|0.1x M KI+0.033(1-x) M K_2SO_4, there is a noticeable dependence of capacitance on the concentration of KI at low frequency range. At $E \geq -0.1$V (vs. Ag|AgCl|ionic liquid) for Bi(111)|ionic liquid systems there can be seen also dependence of capacitance on the concentration of RTIL ions in acetonitrile solutions. Phase angle values increase with c_{KI} from -50° to -65° on both Bi single crystal planes studied, indicating the rise of the role of the adsorption step in the adsorption kinetics, but the limiting stage has still a mixed kinetic nature (diffusion, adsorption and partial charge transfer). At low ac frequency range the phase angle values depend on the ionic liquid chemical composition and the values of phase angle change from -48° (EMImFAP) to -60° ($EMImBF_4$). Thus, the adsorption is likewise limited by mixed kinetics. The slow adsorption stage is observed only in the medium ac frequencies – in frequency range from 1Hz to 100Hz.

6.3.2 Similarity and analysis of Nyquist plots

Analysis of experimentally measured Nyquist plots show that the impedance data for Bi(*hkl*) electrode in both electrolytes, i.e. in the electrolyte aqueous solutions and ionic liquids can be fitted with the modified Frumkin – Melik-Gaikazyan (FMG) equivalent circuit (Fig. 1 (c)), which takes into account the adsorption and diffusion-like mass transfer limited processes at Bi(*hkl*)|electrolyte interfaces.

The electrolyte resistance R_{el} calculated is independent of the electrode potential in the cases of ionic liquids and iodide adsorption at Bi(111) from aqueous solution. There is only a weak dependence of R_{el} on the concentration of the surface active component (KI) at Bi(*hkl*) in the mixed electrolyte solution with constant ionic strength, because the limiting molar conductivity of KI is somewhat higher than that for KF.

The limiting diffusion resistance, R_D, has maximum values in the potential region where the specific adsorption of iodide ions starts in the case of adsorption of iodide ions at Bi(111) and Bi(001) single crystal electrodes or where adsorption of BF_4^- or TCB^- anions from ionic liquid takes place. It can be explained by the reversible partial charge transfer from ions to the electrode surface [5,6, 31–33]. R_D values are independent of the concentration of KI, but there is a dependence of R_D on the crystallographic structure of Bi planes studied. R_D values are lower for more active Bi(001) plane. R_D for Bi(111)|ionic liquid interface depends on the ionic liquid studied and has higher values for $EMImBF_4$ than these for EMImFAP or EMImTCB ionic liquids.

The double layer capacitance C_{dl} depends noticeably on the system studied. In the case of iodide adsorption at Bi(*hkl*) there is a considerable dependence of the electrical double layer capacitance on the electrode potential where the specific adsorption of I^- starts. C_{dl} increases with the concentration of KI in the electrolyte solution with constant ionic strength [23, 31–33]. In ionic liquid systems C_{dl} is practically independent of the electrode potential, because there is no remarkable specific adsorption at Bi(111) single crystal electrode in the high frequency ac region investigated.

Adsorption capacitance C_{ad} values measured in ionic liquids at Bi(111) plane are noticeably lower than these in aqueous solutions, containing KI and KF. The values of C_{ad} show some expansion at less negative electrode potentials for $0.1x$ M KI+$0.1(1\text{-}x)$ M KF and $0.1x$ M KI+$0.033(1\text{-}x)$ M K_2SO_4 systems, which can be explained by the intensive adsorption of iodide ions at Bi(*hkl*) surface. At Bi(001) and at $E>-0.7$ V, the dependence on c_{KI} can be seen, contrary to Bi(111), which is a less active electrode surface.

7. SUMMARY

Cyclic voltammetry and impedance spectroscopy methods have been applied for investigation of the adsorption kinetics of I^- ions at Bi(001) and Bi(111) single crystal plane electrodes in aqueous solutions with constant ionic strength. Electrical double layer structure at Bi(111) in 1-ethyl-3-methyl imidazolium tris(pentafluoroethyl)trifluorophosphate (EMImFAP), 1-ethyl-3-methyl imidazolium tetracyanoborate (EMImTCB) and 1-ethyl-3-methyl imidazolium tetrafluoroborate ($EMImBF_4$) ionic liquids has been studied as well. Experimental data show that the reproducible data in aqueous solution and in ionic liquids can be obtained in the range of ac frequencies from 0.1 to 10000 Hz. It was demonstrated that the Bi(001) electrode is ideally polarizable within the potential region from –1.4 V to –0.5 V (vs. Ag|AgCl|4M KCl) in the aqueous solution with constant ionic strength $0.1x$ M KI + $0.1(1\text{-}x)$ M KF. The Bi(111) single crystal electrode is ideally polarizable in the region from –0.9 to 0.1 V in EMImFAP, from –1.1 to 0.0 V in $EMImBF_4$ and EMImTCB and from –1.4 to –0.55 V (vs. Ag|AgCl|4M KCl) in the aqueous solution of $0.1x$ M KI+$0.033(1\text{-}x)$ M K_2SO_4.

Calculated Nyquist plots by using the various equivalent circuits were fitted to the experimental ones, but the best results were obtained with the modified Frumkin- Melik- Gaikazyan model, where general finite-length diffusion impedance has been introduced into the equivalent circuit. The electrical double layer capacitance, adsorption capacitance, diffusion resistance and other adsorption characteristics depend on the electrode potential applied, as well as on the composition of electrolyte studied.

Analysis of phase angle vs. ac frequency curves shows that adsorption of ions from aqueous medium is limited by mixed kinetics (slow adsorption, diffusion and partial charge transfer steps) at very low ac frequency, as well as from ionic liquids measured. However, mainly the rate of adsorption step is limiting at moderate frequencies from 10 to 200 Hz and electrode potentials, where the specific adsorption of anions starts.

8. REFERENCES

[1] T. Pajkossy, T. Wandlowski, D. M. Kolb, J. Electroanal. Chem., 414 (1996) 209.
[2] V. D. Jovic, B.M. Jovic, J. Electroanal. Chem. 541 (2003) 1.
[3] V. D Jovic, P. Parsons, B. M. Jovic J. Electroanal. Chem. 339 (1992) 327.
[4] T. Langkau, H. Baltruschat, Electrochim. Acta 44 (1998) 909.
[5] M. Väärtnõu, E. Lust, J. Electroanal. Chem. 533 (2002) 107.
[6] M. Väärtnõu and E. Lust, J. Electroanal. Chem. 565 (2004) 211.
[7] D. Eberhardt, E. Santos, W. Schmickler, J. Electroanal. Chem. 419 (1996) 23.
[8] G. Beltramo, E. Santos, J. Electroanal. Chem. 556 (2003) 127.
[9] A.N. Frumkin, Potentials of Zero Charge, Moscow, Nauka, 1979 (in Russian).
[10] O. Magnussen, Chem. Rev. 102 (2002) 679.
[11] B. Jović, V.D. Jović, D.M. Dražić, J. Electroanal. Chem. 399 (1995) 197.
[12] K. Bange, B. Straehler, J.K. Sass, J. Electroanal. Chem. 299 (1987) 87.
[13] M.S. Zei, J. Electroanal. Chem. 308 (1991) 295.
[14] G. Aloisi, A.M. Funtikov, T. Will, J. Electroanal. Chem. 370 (1994) 297.
[15] M.L. Foresti, G. Aloisi, M. Innocenti, H. Kobayashi, R. Guidelli, Surf. Sci 335 (1995) 241.
[16] M. Koper, J. Electroanal. Chem. 450 (1998) 189.
[17] S. Mitshell, G. Brown, P. Riktvold, Surf. Sci. 471 (2001) 125.
[18] R. Parsons, Trans. Faraday Soc. 51 (1955) 1518.
[19] Z. Shi, S. Wu, J. Lipkowski, J. Electroanal. Chem. 384 (1995) 171.
[20] Z. Shi, J. Lipkowski, J. Electroanal. Chem. 403 (1996) 225.
[21] W. Schmickler, Interfacial Electrochemistry, Oxford University Press, New York, 1996.
[22] S. Kallip and E. Lust, Electrochem. Communications 7 (2005) 863.
[23] E. Lust, in A. J. Bard, M. Stratman: Encyclopedia of Electrochemistry, Vol. 1, Wiley, 2002, p. 188.
[24] B. Damaskin, S. Karpov, S. Dyatkina, U. Palm and M. Salve, J. Electroanal. Chem. 189 (1985) 183.
[25] B. Damaskin, I. Pankratova, U. Palm, K. Anni, M. Väärtnõu and M. Salve, J. Electroanal. Chem. 234 (1987) 31.
[26] B. Damaskin, U. Palm and M. Salve, J. Electroanal. Chem. 218 (1987) 65.
[27] M.A. Vorotyntsev and K. Golub, Elektrokhimiya 29 (1984) 256.
[28] M.A. Vorotyntsev, Itogi nauki i tekhniki. Elektrokhimiya 26 (1988) 3.
[29] J.W. Schultze and K.J. Vetter, J. Electroanal. Chem. 44 (1973) 63.
[30] W. Schmickler and R. Guidelli, J. Electroanal.Chem. 235 (1987) 387.
[31] K. Lust, M. Väärtnõu and E. Lust, Electrochimica Acta, 45 (2000) 3543.
[32] K. Lust, M. Väärtnõu and E. Lust, J. Electroanal. Chem. 532 (2002) 303.
[33] K. Lust, E. Lust, J. Electroanal. Chem. 552 (2003) 129.
[34] M.Väärtnõu, E.Lust, J. Electroanal. Chem. 578 (2005) 273.
[35] W. Liu, L. Cheng, Y. Zhang, H. Wang, M. Yu, Journal of Molecular Liquids 140 (2008) 68.
[36] F. Endres, S. Abedin, Phys. Chem. Chem. Phys. 8 (2006) 2101.
[37] R.J. Gale, R.A. Osteryoung, Electrochim. Acta, 25 (1980) 1527.
[38] T. Welton, Chem.Rev. 99 (1999) 2071.
[39] P. Wasserschied, W. Keim, Angew. Chem., Int. Ed. 39 (2000) 3772.
[40] M.J. Earle, K.R. Seddon, Pure Appl. Chem. 72 (2000) 1391.
[41] M. Galinski, A. Lewandowski, I. Stepniak, Electrochim. Acta 51 (2006) 5567.

[42] H. Matsumoto, in Electrochemical Aspects of Ionic Liquids, H. Ohno, Editor, John Wiley & Sons, Inc., New Jersey (2005).
[43] S. Takahashi, N. Koura, S. Kobara, M.-L. Saboungi, L.A. Curtiss, Plasmas and Ions 2 (1999) 91.
[44] J.L. Anderson, D.W. Armstrong, G.-T. Wei, Anal. Chem. 78 (2006) 2892 .
[45] M.C. Buzzero, R.G. Evans, R.G. Compton, Chem. Phys. Phys. Chem. 5 (2004) 1105.
[46] R. Hagiwara, Y. Ho, J. Fluorine Chem. 105 (2000) 221.
[47] A.A. Kornyshev, J. Phys. Chem. 111 (2007) 5545.
[48] A. A. Kornyshev, J. Phys. Chem, B, 612 (2008) 11868.
[49] M. Biso, M. Mastragostino, M. Montanino, S. Passerini, F. Soavi, Electrochim. Acta 53 (2008) 7967.
[50] M. Lazzari, F. Soavi, M. Mastragostino, J. Power Sources 198 (2008) 490.
[51] H. Kurig, A. Jänes, E. Lust, J. Electrochem. Soc. 157 (2010) A272.
[52] H. Liu, G. Zhua, Journal of Power Sources 171 (2007) 1054.
[53] M.V. Fedorov, A.A. Kornyshev, Electrochim. Acta 53 (2008) 6835.
[54] M.J. Earle, K.R. Seddon, Pure Appl. Chem. 72 (2000) 1391.
[55] K.N. Marsh, A. Deev, A.C.-T. Wu, E. Tran, A. Klamt, Kor. J. Chem. Eng. 19 (2002) 357.
[56] P. Wasserscheid, W. Keim, Angew. Chem. Int. Ed. 39 (2000) 3772.
[57] J. S. Wilkes, Journal of Molecular Catalysis A: Chemical 214 (2004) 11.
[58] F. Endres, ChemPhysChem 3 (2002) 144.
[59] H. Matsumoto, H. Sakaebe, K. Tatsumi, J. Power Sources 146 (2005) 45.
[60] H. Sakaebe, H. Matsumoto, K. Tatsumi, J. Power Sources 146 (2005) 693.
[61] M. Egashira, H. Todo, N. Yoshimoto, M. Morita, J. Yamaki, Journal of Power Sources 174 (2007) 560.
[62] M.C. Buzzeo, C. Hardacre, R.G. Compton, Anal. Chem. 76 (2004) 4583.
[63] E. Bakker, M. Telting-Diaz, Anal. Chem. 74 (2002) 2781.
[64] E. Bakker, Anal. Chem. 76 (2004) 3285.
[65] E. Bakker, Y. Qin, Anal. Chem. 78 (2006) 3965.
[66] P. Buhlmann, E. Pretsch, E. Bakker, Chem. Rev. 98 (1998) 1593.
[67] T. Sato, G. Masuda, K. Takagi, Electrochimica Acta 49 (2004) 3603.
[68] A.B. McEwen, H.L. Ngo, K. LeCompte, J.L. Goldman, J. Electrochem. Soc. 146 (1999) 1687.
[69] M. Ue, M. Takeda, J. Korean Electrochem. Soc. 5 (2002) 192.
[70] P. Wang, S.M. Zakeeruddin, J.-E. Moser, M. Grätzel, J. Phys. Chem. B 107 (2003) 13280.
[71] A. Noda, M.A.B.H. Susan, K. Kudu, S. Mitsushima, K. Hayamizu, M. Watanabe, J.Phys. Chem. B 107 (2003) 4024.
[72] J. Padilha, J. Basso, L.G. da Trindade, Emilse M.A. Martini, M. de Souza, R. de Souza, J. Power Sources 195 (2010) 6483.
[73] M. Martinez, Y. Molmeret, L. Cointeaux, C. Iojoiu, J. Leprêtre, N. El Kissi, P. Judeinstein, J. Sanchez, J. Power Sources 195 (2010) 5829.
[74] R. F. de Souza, J. C. Padilha, R. S. Goncalves, J. Dupont, Electrochem.Comm. 5 (2003) 728.
[75] J. Belieres, D. Gervasio, C. Austen Angell, Chem. Commun., (2006) 4799.
[76] A.N. Frumkin, V.I. Melik-Gaikazyan, Dokl. Akad. Nauk SSSR 77 (1951) 855.
[77] B. Ershler, Zh. Fiz. Khim. USSR 22 (1948) 683.
[78] M. Sluyters-Rehbach, J. H. Sluyters, in A. J. Bard, Electroanalytical Chemistry, Vol. 4, Marcel Dekker, New York, 1970, p. 1.

[79] A. Lasia, in B.E. Conway, J. O'M. Bockris, R.E. White (Eds.), Modern Aspects of Electrochemistry, Vol 32, Kluwer Academic / Plenum Publishers, New York, 1999, p 143.

[80] J.R. Macdonald, W.B. Johnson, in J.R. Macdonald (Ed.), Impedance spectroscopy, Wiley, New York, 1987, p. 1.

[81] Z View for Windows (ver. 2.2), Scribner, Southern Pines, NC, USA.

[82] R.S. Neves, E. De Robertis, A.J. Motheo, Capacitance dispersion in electrochemical impedance spectroscopy measurements of iodide adsorption on Au(1 1 1), Applied Surface Science (online, 2006).

[83] R. Parsons, in: J.O'M. Bockris, B.E. Conway and E. Yeager (Eds.), Comprehensive Treatise of Electrochemistry, Vol 1, Plenum Press, New York, 1981, CR. 1, p. 1.

[84] G. Nurk, A. Jänes, K. Lust, E. Lust, J. Electroanal. Chem. 515 (2001) 17.

[85] A. Jänes, E. Lust, Electrochim. Acta 47 (2001) 967.

[86] S. Trasatti, E. Lust, in Modern Aspects of Electrochemistry, Vol. 33, R.E. White, B.E. Conway, J.O'M. Bockris, Editors, Kluwer Academic/Plenum Publishers, New York and London (1999).

[87] E. Lust, in Encyclopedia of Electrochemistry, Vol. 1, A.J. Bard, M. Stratman, Editors, Wiley (2003).

[88] L. Siinor, K. Lust, E. Lust, J. Electroanal. Chem. 601 (2007) 39.

[89] L. Siinor, K. Lust, E. Lust, ECS Trans. 16 (49) (2009) 559.

[90] W. Lorenz, G. Salie, J. Electroanal. Chem. 80 (1975) 309.

[91] A.A. Kornyshev, J. Phys. Chem. B 111 (2007) 5545.

[92] M.V. Fedorov, A.A. Kornyshev, Electrochim. Acta 53 (2008) 6835.

[93] M.V. Fedorov, M. Georgi, A.A. Kornyshev, Electrochem. Commun. 12 (2010) 296.

[94] E. Barsoukov, J.R. Macdonald, Impedance Spectroscopy. Theory, Experiment and Applications (2nd Ed.), Wiley-Interscience, Hoboken, New Jersey (2005).

[95] H. Kurig, A. Jänes, E. Lust, Electrochemical characteristics of carbide derived carbon | 1-ethyl-e-methylimidazolium tetrafluoroborate electrical double layer characteristics, J. Electrochem. Soc. (1010)

[96] A. Jänes, E. Lust, Electrochem. Commun. 7 (2005) 510.

[97] M. Arulepp, J. Leis, M. Lätt, F. Miller, K. Rumma, E. Lust, A. Burke, J. Power Sources 135 (2006) 1460.

9. SUMMARY IN ESTONIAN

Ioonide adsorptsioonikineetika Bi monokristalli tahkudel vesilahustes ja ioonsetes vedelikes

Antud töös uuriti elektrokeemilise impedantsspektroskoopia meetodiga jodiidiooni adsorptsioonikineetikat järgmistes süsteemides: Bi(001) | 0.1 xM KI + 0.1 (1-x) M KF, kus x on KI moolmurd, mille puhul elektrood on ideaalselt polariseeritav potentsiaalivahemikus –1.4V kuni –0.5 V (vs. Ag|AgCl|4M KCl), Bi(111) | 0.1x M KI+0.033(1-x) M K_2SO_4, kus x on KI moolmurd ning ideaalse polariseeritavuse ala on –1.3V kuni –0.5V (vs. Ag|AgCl|4M KCl). Ioonse vedeliku ja Bi(111) piirpinnale tekkiva elektrilise kaksikkihi parameetreid uuriti lisaks elektrokeemilisele impedantsspektroskoopiale ka tsüklilise voltamperomeetria meetodiga järgmistes ioonsetes vedelikes: 1-etüül-3-metüül-imidasoolium tetrafluoroboraat ($EMImBF_4$), 1-etüül-3-metüül-imidasoolium tris(pentafluoroetüül)trifluorofosfaat (EMImFAP), 1-etüül-3-metüül-imidasoolium tetratsüaanoboraat (EMImTCB). Bi(111) on $EMImBF_4$ and EMImTCB korral ideaalselt polariseeritav –1.1 kuni 0.0 V (vs. Ag|AgCl|RTIL) ning EMImFAP puhul –0.9 kuni 0.1 V (vs. Ag|AgCl|RTIL). Enne iga eksperimenti poleeriti vismutelektrood elektrokeemiliselt KI+HCl lahuses. Mõõtmised ioonsetes vedelikes viidi läbi kuivkapis (Labmaster sp, LMBraun; O_2 and H_20 concentrations <0.1 ppm) argooni (99.99995%) keskkonnas.

Eksperimentaalselt mõõdetud reaktiivtakistuse Z'' ja aktiivtakistuse Z' sõltuvuste mittelineaarne regressioonanalüüs näitas, et kõigi mõõdetud süsteemide puhul andis paremaid modelleerimistulemusi klassikalise Frumkin- Melik-Gaikazyani mudel, kuigi andmeid modelleeriti ka teiste ekvivalentskeemidega. Modelleerimistulemuste kokkulangevust eksperimentaalsete andmetega analüüsiti mittelineaarse regressioonanalüüsi abil määratud χ^2- funktsiooni ja kaalutud ruutkeskmine hälbe põhjal ning üksikute parameetrite väärtuste ja nende standardhälvete põhjal. Faasinurga vahelduvvoolu sagedusest sõltuvused näitasid, et jodiidiooni adsorptsiooni kiirust määravad staadiumid (vahetu adsorptsioon, osakeste difusioon pinnale ning osaline laenguülekanne) on võrreldavate kiirustega ning suuremal osal uuritud vahelduvvoolu sageduste alas allub I^- adsorptsiooniprotsess segakineetika seaduspärasustele. Tehti kindlaks, et KF ega K_2SO_4 vesilahuste korral ei sõltu vahelduvvoolu faasinurk elektroodipotentsiaalist, küll aga on näha faasinurga sõltuvust potentsiaalist KI lahuses nii vahelduvvoolu kõrgsageduslikus kui ka madalsageduslikus alas, mis näitab, et jodiidioonid adsorbeeruvad Bi(001) ning Bi(111) elektroodil spetsiifiliselt ning adsorptsiooniprotsess on uuritud potentsiaalide vahemikus kiire ning pöörduv. Bi(111)|ioonne vedelik süsteemides oli näha sarnast käitumist, ehk siis suuremal osal uuritud sageduste alas protsess on limiteeritud segakineetika poolt (vahetu adsorptsioon, osakeste difusioon pinnale ning osaline laenguülekanne), kuigi faasinurga vahelduvvoolu sagedusest sõltuvuste kuju on mõnevõrra erinev ioonsete vedelike puhul, mida antud töös uuriti.

10. ACKNOWLEDGEMENTS

The process of completing this work has left me indebted to several people. I would like to express my deepest gratitude towards them.

First I would like to thank my supervisors Professor Enn Lust and Karmen Lust for their invaluable comments, guidance and support during all these years of our collaboration. Also for providing me a working environment in which I was able to finish these theses.

Thanks go to my colleagues for encouragement, I am grateful for all these inspiring discussions over the years.

I wish to thank my friends for friendship that we have shared through all these years, also for advice and being there for me on more occasions than I can count.

My guileless thanks go to my grandmother and brother for their support, forbearance and understanding.

11. PUBLICATIONS

CURRICULUM VITAE

Liis Siinor

Born: 12.07 1982, Saaremaa, Estonia
Citizenship: Estonian
Address: Institute of Chemistry
University of Tartu
14A Ravila St., Tartu 50411, Estonia
E-mail: liis.siinor@ut.ee

Education

2006–...	University of Tartu, *Ph.D.* student (physical and electrochemistry)
2004–2006	University of Tartu, *M.Sc.* in physical and electrochemistry
2000–2004	University of Tartu, *B.Sc.* in chemistry

Professional employmant

2007–2008	University of Tartu, Doctoral School of Material Science and Material Technology, researcher (0.1).
2004–...	University of Tartu, Institute of Chemistry, laboratorian.

List of publications

1. L. Siinor, K. Lust, E. Lust, Influence of anion composition and size on the double layer capacitance for Bi(111) | room temperature ionic liquid interface, Electrochemistry Communications, Article in Press.
2. L. Siinor, K. Lust, E. Lust, Electrical Double Layer Capacitance at Bi(111)|1-Ethyl-3-methylimidazolium Tetrafluoroborate Interface as a Function of the Electrode Potential, Journal of Electrochemical Society, Volume 157, Issue 7, 25 May 2010, Pages F83–F87.
3. L. Siinor, V. Ivaništšev, K. Lust, E. Lust, Impedance study of adsorption of iodide ions at Cd(0001) and Bi(111) electrode from various solutions with constant ionic strength, Journal of Solid State Electrochemistry, Volume 14, Number 4, April, 2010, Pages 555–563.
4. L. Siinor, K. Lust, E. Lust, Ionic liquids and their electrochemical behavior at Bi(111) single crystal electrode, In: Abstracts of Scientific Conference: 31th Estonian Chemistry Days, Tallinn, Estonia, April 28, 2010.

5. L. Siinor, K. Lust, E. Lust, Electrochemical characteristics of Bi(111) electrode in ionic liquids, FMTDK conference, Tartu, Estonia, February 25–26, 2010.
6. L. Siinor, H. Kurig, A. Jänes, K. Lust and E. Lust, Electrochemical Characteristics of Bi(111) and Nanoporous Carbon Electrodes in Ionic Liquids, 217th ECS Meeting, Vancouver, Canada, April 28, 2010.
7. L. Siinor, K. Lust, and E. Lust, Electrical Double Layer Structure at Bi(111)|1-ethyl-3-methyl-imidazolium Tetrafluoroborate Interface, ECS Transactions, Volume 16 , Issue 49, October 2008, Pages 559–567.
8. L. Siinor, K. Lust and E. Lust, Electrical Double Layer Structure at Bi(111)|1-ethyl-3-methyl-imidazolium Tetrafluoroborate Interface, 214th ECS Meeting, Honolulu, USA, 2008.
9. L. Siinor, K. Lust, Adsorption kinetics of iodide ions on the bismuth single crystal planes from different base electrolyte solutions, In: 5th Baltic Conference on Electrochemistry, Tartu, Estonia, 2008, P-33.
10. L. Siinor, K. Lust, E. Lust, Electrical Double Layer Structure at Bi(111) | 1-ethyl-3-methylimidazolium tetrafluoroborate interface, In: 5th Baltic Conference on Electrochemistry, Tartu, Estonia, 2008, P-52.
11. L. Siinor, K. Lust, E. Lust, Adsorption kinetics of iodide ion at Bi(001) in several surface inactive electrolytes, In: Abstracts of Scientific Conference: 30th Estonian Chemistry Days, Tartu, Eesti, 2007, P-73.
12. L. Siinor, K. Lust and E. Lust, Impedance study of adsorption of iodide ions at Bi(001) electrode from the aqueous solutions with constant ionic strength, Journal of Electroanalytical Chemistry, Volume 601, Issues 1–2, 15 March 2007, Pages 39–46.
13. L. Siinor, K. Lust, E. Lust, Adsorption kinetics of iodide anions on bismuth single crystal planes, In: Abstracts of: the 57th Annual Meeting of international Society of Electrochemistry, Edinburgh, UK, 2006, S8. P-73.
14. K. Lust, L.Siinor, M. Väärtnõu, Adsorption kinetics of bromide ions on the electrochemically polished Cd(0001) plane, In: Abstracts of: the 55th Annual Meeting of international Society of Electrochemistry, Thessaloniki, Greece, 2004, p.62.

ELULOOKIRJELDUS

Liis Siinor

Sünniaeg ja koht: 12.07 1982, Saaremaa, Eesti
Kodakondsus: Eesti
Aadress: Keemia Instituut
Tartu Ülikool
Ravila 14A, Tartu 50411, Eesti
E-mail: liis.siinor@ut.ee

Haridus

2006–...	Tartu Ülikool, *Ph.D.* (füüsikalise ja elektrokeemia erialal)
2004–2006	Tartu Ülikool, *M.Sc.* (füüsikalise ja elektrokeemia erialal)
2000–2004	Tartu Ülikool, *B.Sc.* (keemia erialal)

Teenistuskäik

2007–2008	Tartu Ülikool, Materjaliteaduse ja materjalide tehnoloogia doktorikool (0.1)
2004–...	Tartu Ülikool, Keemia instituut, laborant

Ilmunud publikatsioonid

1. L. Siinor, K. Lust, E. Lust, Influence of anion composition and size on the double layer capacitance for Bi(111) | room temperature ionic liquid interface, Electrochemistry Communications, Article in Press.
2. L. Siinor, K. Lust, E. Lust, Electrical Double Layer Capacitance at Bi(111)|1-Ethyl-3-methylimidazolium Tetrafluoroborate Interface as a Function of the Electrode Potential, Journal of Electrochemical Society, Volume 157, Issue 7, 25 May 2010, Pages F83–F87.
3. L. Siinor, V. Ivaništšev, K. Lust, E. Lust, Impedance study of adsorption of iodide ions at Cd(0001) and Bi(111) electrode from various solutions with constant ionic strength, Journal of Solid State Electrochemistry, Volume 14, Number 4, April, 2010, Pages 555–563.
4. L. Siinor, K. Lust, E. Lust, Ionic liquids and their electrochemical behavior at Bi(111) single crystal electrode, In: Abstracts of Scientific Conference: 31th Estonian Chemistry Days, Tallinn, Estonia, April 28, 2010.
5. L. Siinor, K. Lust, E. Lust, Electrochemical characteristics of Bi(111) electrode in ionic liquids, FMTDK conference, Tartu, Estonia, February 25–26, 2010.

6. L. Siinor, H. Kurig, A. Jänes, K. Lust and E. Lust, Electrochemical Characteristics of Bi(111) and Nanoporous Carbon Electrodes in Ionic Liquids, 217th ECS Meeting, Vancouver, Canada, April 28, 2010.
7. L. Siinor, K. Lust, and E. Lust, Electrical Double Layer Structure at Bi(111)|1-ethyl-3-methyl-imidazolium Tetrafluoroborate Interface, ECS Transactions, Volume 16 , Issue 49, October 2008, Pages 559–567.
8. L. Siinor, K. Lust and E. Lust, Electrical Double Layer Structure at Bi(111)|1-ethyl-3-methyl-imidazolium Tetrafluoroborate Interface, 214th ECS Meeting, Honolulu, USA, 2008.
9. L. Siinor, K. Lust, Adsorption kinetics of iodide ions on the bismuth single crystal planes from different base electrolyte solutions, In: 5th Baltic Conference on Electrochemistry, Tartu, Estonia, 2008, P-33.
10. L. Siinor, K. Lust, E. Lust, Electrical Double Layer Structure at Bi(111) | 1-ethyl-3-methylimidazolium tetrafluoroborate interface, In: 5th Baltic Conference on Electrochemistry, Tartu, Estonia, 2008, P-52.
11. L. Siinor, K. Lust, E. Lust, Adsorption kinetics of iodide ion at Bi(001) in several surface inactive electrolytes, In: Abstracts of Scientific Conference: 30th Estonian Chemistry Days, Tartu, Eesti, 2007, P-73.
12. L. Siinor, K. Lust and E. Lust, Impedance study of adsorption of iodide ions at Bi(001) electrode from the aqueous solutions with constant ionic strength, Journal of Electroanalytical Chemistry, Volume 601, Issues 1–2, 15 March 2007, Pages 39–46.
13. L. Siinor, K. Lust, E. Lust, Adsorption kinetics of iodide anions on bismuth single crystal planes, In: Abstracts of: the 57th Annual Meeting of international Society of Electrochemistry, Edinburgh, UK, 2006, S8.P-73.
14. K. Lust, L.Siinor, M. Väärtnõu, Adsorption kinetics of bromide ions on the electrochemically polished Cd(0001) plane, In: Abstracts of: the 55th Annual Meeting of international Society of Electrochemistry, Thessaloniki, Greece, 2004, p.62.

DISSERTATIONES CHIMICAE UNIVERSITATIS TARTUENSIS

1. **Toomas Tamm.** Quantum-chemical simulation of solvent effects. Tartu, 1993, 110 p.
2. **Peeter Burk.** Theoretical study of gas-phase acid-base equilibria. Tartu, 1994, 96 p.
3. **Victor Lobanov.** Quantitative structure-property relationships in large descriptor spaces. Tartu, 1995, 135 p.
4. **Vahur Mäemets.** The ^{17}O and ^{1}H nuclear magnetic resonance study of H_2O in individual solvents and its charged clusters in aqueous solutions of electrolytes. Tartu, 1997, 140 p.
5. **Andrus Metsala.** Microcanonical rate constant in nonequilibrium distribution of vibrational energy and in restricted intramolecular vibrational energy redistribution on the basis of slater's theory of unimolecular reactions. Tartu, 1997, 150 p.
6. **Uko Maran.** Quantum-mechanical study of potential energy surfaces in different environments. Tartu, 1997, 137 p.
7. **Alar Jänes.** Adsorption of organic compounds on antimony, bismuth and cadmium electrodes. Tartu, 1998, 219 p.
8. **Kaido Tammeveski.** Oxygen electroreduction on thin platinum films and the electrochemical detection of superoxide anion. Tartu, 1998, 139 p.
9. **Ivo Leito.** Studies of Brønsted acid-base equilibria in water and non-aqueous media. Tartu, 1998, 101 p.
10. **Jaan Leis.** Conformational dynamics and equilibria in amides. Tartu, 1998, 131 p.
11. **Toonika Rinken.** The modelling of amperometric biosensors based on oxidoreductases. Tartu, 2000, 108 p.
12. **Dmitri Panov.** Partially solvated Grignard reagents. Tartu, 2000, 64 p.
13. **Kaja Orupõld.** Treatment and analysis of phenolic wastewater with microorganisms. Tartu, 2000, 123 p.
14. **Jüri Ivask.** Ion Chromatographic determination of major anions and cations in polar ice core. Tartu, 2000, 85 p.
15. **Lauri Vares.** Stereoselective Synthesis of Tetrahydrofuran and Tetrahydropyran Derivatives by Use of Asymmetric Horner-Wadsworth-Emmons and Ring Closure Reactions. Tartu, 2000, 184 p.
16. **Martin Lepiku.** Kinetic aspects of dopamine D_2 receptor interactions with specific ligands. Tartu, 2000, 81 p.
17. **Katrin Sak.** Some aspects of ligand specificity of P2Y receptors. Tartu, 2000, 106 p.
18. **Vello Pällin.** The role of solvation in the formation of iotsitch complexes. Tartu, 2001, 95 p.

19. **Katrin Kollist.** Interactions between polycyclic aromatic compounds and humic substances. Tartu, 2001, 93 p.
20. **Ivar Koppel.** Quantum chemical study of acidity of strong and superstrong Brønsted acids. Tartu, 2001, 104 p.
21. **Viljar Pihl.** The study of the substituent and solvent effects on the acidity of OH and CH acids. Tartu, 2001, 132 p.
22. **Natalia Palm.** Specification of the minimum, sufficient and significant set of descriptors for general description of solvent effects. Tartu, 2001, 134 p.
23. **Sulev Sild.** QSPR/QSAR approaches for complex molecular systems. Tartu, 2001, 134 p.
24. **Ruslan Petrukhin.** Industrial applications of the quantitative structure-property relationships. Tartu, 2001, 162 p.
25. **Boris V. Rogovoy.** Synthesis of (benzotriazolyl)carboximidamides and their application in relations with *N*- and *S*-nucleophyles. Tartu, 2002, 84 p.
26. **Koit Herodes.** Solvent effects on UV-vis absorption spectra of some solvatochromic substances in binary solvent mixtures: the preferential solvation model. Tartu, 2002, 102 p.
27. **Anti Perkson.** Synthesis and characterisation of nanostructured carbon. Tartu, 2002, 152 p.
28. **Ivari Kaljurand.** Self-consistent acidity scales of neutral and cationic Brønsted acids in acetonitrile and tetrahydrofuran. Tartu, 2003, 108 p.
29. **Karmen Lust.** Adsorption of anions on bismuth single crystal electrodes. Tartu, 2003, 128 p.
30. **Mare Piirsalu.** Substituent, temperature and solvent effects on the alkaline hydrolysis of substituted phenyl and alkyl esters of benzoic acid. Tartu, 2003, 156 p.
31. **Meeri Sassian.** Reactions of partially solvated Grignard reagents. Tartu, 2003, 78 p.
32. **Tarmo Tamm.** Quantum chemical modelling of polypyrrole. Tartu, 2003. 100 p.
33. **Erik Teinemaa.** The environmental fate of the particulate matter and organic pollutants from an oil shale power plant. Tartu, 2003. 102 p.
34. **Jaana Tammiku-Taul.** Quantum chemical study of the properties of Grignard reagents. Tartu, 2003. 120 p.
35. **Andre Lomaka.** Biomedical applications of predictive computational chemistry. Tartu, 2003. 132 p.
36. **Kostyantyn Kirichenko.** Benzotriazole — Mediated Carbon–Carbon Bond Formation. Tartu, 2003. 132 p.
37. **Gunnar Nurk.** Adsorption kinetics of some organic compounds on bismuth single crystal electrodes. Tartu, 2003, 170 p.
38. **Mati Arulepp.** Electrochemical characteristics of porous carbon materials and electrical double layer capacitors. Tartu, 2003, 196 p.

39. **Dan Cornel Fara.** QSPR modeling of complexation and distribution of organic compounds. Tartu, 2004, 126 p.
40. **Riina Mahlapuu.** Signalling of galanin and amyloid precursor protein through adenylate cyclase. Tartu, 2004, 124 p.
41. **Mihkel Kerikmäe.** Some luminescent materials for dosimetric applications and physical research. Tartu, 2004, 143 p.
42. **Jaanus Kruusma.** Determination of some important trace metal ions in human blood. Tartu, 2004, 115 p.
43. **Urmas Johanson.** Investigations of the electrochemical properties of polypyrrole modified electrodes. Tartu, 2004, 91 p.
44. **Kaido Sillar.** Computational study of the acid sites in zeolite ZSM-5. Tartu, 2004, 80 p.
45. **Aldo Oras.** Kinetic aspects of dATPαS interaction with $P2Y_1$ receptor. Tartu, 2004, 75 p.
46. **Erik Mölder.** Measurement of the oxygen mass transfer through the air-water interface. Tartu, 2005, 73 p.
47. **Thomas Thomberg.** The kinetics of electroreduction of peroxodisulfate anion on cadmium (0001) single crystal electrode. Tartu, 2005, 95 p.
48. **Olavi Loog.** Aspects of condensations of carbonyl compounds and their imine analogues. Tartu, 2005, 83 p.
49. **Siim Salmar.** Effect of ultrasound on ester hydrolysis in aqueous ethanol. Tartu, 2006, 73 p.
50. **Ain Uustare.** Modulation of signal transduction of heptahelical receptors by other receptors and G proteins. Tartu, 2006, 121 p.
51. **Sergei Yurchenko.** Determination of some carcinogenic contaminants in food. Tartu, 2006, 143 p.
52. **Kaido Tämm.** QSPR modeling of some properties of organic compounds. Tartu, 2006, 67 p.
53. **Olga Tšubrik.** New methods in the synthesis of multisubstituted hydrazines. Tartu. 2006, 183 p.
54. **Lilli Sooväli.** Spectrophotometric measurements and their uncertainty in chemical analysis and dissociation constant measurements. Tartu, 2006, 125 p.
55. **Eve Koort.** Uncertainty estimation of potentiometrically measured ph and pK_a values. Tartu, 2006, 139 p.
56. **Sergei Kopanchuk.** Regulation of ligand binding to melanocortin receptor subtypes. Tartu, 2006, 119 p.
57. **Silvar Kallip.** Surface structure of some bismuth and antimony single crystal electrodes. Tartu, 2006, 107 p.
58. **Kristjan Saal.** Surface silanization and its application in biomolecule coupling. Tartu, 2006, 77 p.
59. **Tanel Tätte.** High viscosity $Sn(OBu)_4$ oligomeric concentrates and their applications in technology. Tartu, 2006, 91 p.

60. **Dimitar Atanasov Dobchev**. Robust QSAR methods for the prediction of properties from molecular structure. Tartu, 2006, 118 p.
61. **Hannes Hagu**. Impact of ultrasound on hydrophobic interactions in solutions. Tartu, 2007, 81 p.
62. **Rutha Jäger.** Electroreduction of peroxodisulfate anion on bismuth electrodes. Tartu, 2007, 142 p.
63. **Kaido Viht.** Immobilizable bisubstrate-analogue inhibitors of basophilic protein kinases: development and application in biosensors. Tartu, 2007, 88 p.
64. **Eva-Ingrid Rõõm.** Acid-base equilibria in nonpolar media. Tartu, 2007, 156 p.
65. **Sven Tamp.** DFT study of the cesium cation containing complexes relevant to the cesium cation binding by the humic acids. Tartu, 2007, 102 p.
66. **Jaak Nerut.** Electroreduction of hexacyanoferrate(III) anion on Cadmium (0001) single crystal electrode. Tartu, 2007, 180 p.
67. **Lauri Jalukse.** Measurement uncertainty estimation in amperometric dissolved oxygen concentration measurement. Tartu, 2007, 112 p.
68. **Aime Lust.** Charge state of dopants and ordered clusters formation in CaF_2:Mn and CaF_2:Eu luminophors. Tartu, 2007, 100 p.
69. **Iiris Kahn**. Quantitative Structure-Activity Relationships of environmentally relevant properties. Tartu, 2007, 98 p.
70. **Mari Reinik.** Nitrates, nitrites, N-nitrosamines and polycyclic aromatic hydrocarbons in food: analytical methods, occurrence and dietary intake. Tartu, 2007, 172 p.
71. **Heili Kasuk.** Thermodynamic parameters and adsorption kinetics of organic compounds forming the compact adsorption layer at Bi single crystal electrodes. Tartu, 2007, 212 p.
72. **Erki Enkvist.** Synthesis of adenosine-peptide conjugates for biological applications. Tartu, 2007, 114 p.
73. **Svetoslav Hristov Slavov**. Biomedical applications of the QSAR approach. Tartu, 2007, 146 p.
74. **Eneli Härk.** Electroreduction of complex cations on electrochemically polished Bi(*hkl*) single crystal electrodes. Tartu, 2008, 158 p.
75. **Priit Möller.** Electrochemical characteristics of some cathodes for medium temperature solid oxide fuel cells, synthesized by solid state reaction technique. Tartu, 2008, 90 p.
76. **Signe Viggor.** Impact of biochemical parameters of genetically different pseudomonads at the degradation of phenolic compounds. Tartu, 2008, 122 p.
77. **Ave Sarapuu.** Electrochemical reduction of oxygen on quinone-modified carbon electrodes and on thin films of platinum and gold. Tartu, 2008, 134 p.
78. **Agnes Kütt.** Studies of acid-base equilibria in non-aqueous media. Tartu, 2008, 198 p.

79. **Rouvim Kadis.** Evaluation of measurement uncertainty in analytical chemistry: related concepts and some points of misinterpretation. Tartu, 2008, 118 p.
80. **Valter Reedo.** Elaboration of IVB group metal oxide structures and their possible applications. Tartu, 2008, 98 p.
81. **Aleksei Kuznetsov.** Allosteric effects in reactions catalyzed by the cAMP-dependent protein kinase catalytic subunit. Tartu, 2009, 133 p.
82. **Aleksei Bredihhin.** Use of mono- and polyanions in the synthesis of multisubstituted hydrazine derivatives. Tartu, 2009, 105 p.
83. **Anu Ploom.** Quantitative structure-reactivity analysis in organosilicon chemistry. Tartu, 2009, 99 p.
84. **Argo Vonk.** Determination of adenosine A_{2A}- and dopamine D_1 receptor-specific modulation of adenylate cyclase activity in rat striatum. Tartu, 2009, 129 p.
85. **Indrek Kivi.** Synthesis and electrochemical characterization of porous cathode materials for intermediate temperature solid oxide fuel cells. Tartu, 2009, 177 p.
86. **Jaanus Eskusson.** Synthesis and characterisation of diamond-like carbon thin films prepared by pulsed laser deposition method. Tartu, 2009, 117 p.
87. **Margo Lätt.** Carbide derived microporous carbon and electrical double layer capacitors. Tartu, 2009, 107 p.
88. **Vladimir Stepanov.** Slow conformational changes in dopamine transporter interaction with its ligands. Tartu, 2009, 103 p.
89. **Aleksander Trummal.** Computational Study of Structural and Solvent Effects on Acidities of Some Brønsted Acids. Tartu, 2009, 103 p.
90. **Eerold Vellemäe.** Applications of mischmetal in organic synthesis. Tartu, 2009, 93 p.
91. **Sven Parkel.** Ligand binding to 5-HT_{1A} receptors and its regulation by Mg^{2+} and Mn^{2+}. Tartu, 2010, 99 p.
92. **Signe Vahur.** Expanding the possibilities of ATR-FT-IR spectroscopy in determination of inorganic pigments. Tartu, 2010, 184 p.
93. **Tavo Romann**. Preparation and surface modification of bismuth thin film, porous, and microelectrodes. Tartu, 2010, 155 p.
94. **Nadežda Aleksejeva.** Electrocatalytic reduction of oxygen on carbon nanotube-based nanocomposite materials. Tartu, 2010, 147 p.
95. **Marko Kullapere.** Electrochemical properties of glassy carbon, nickel and gold electrodes modified with aryl groups. Tartu, 2010, 233 p.